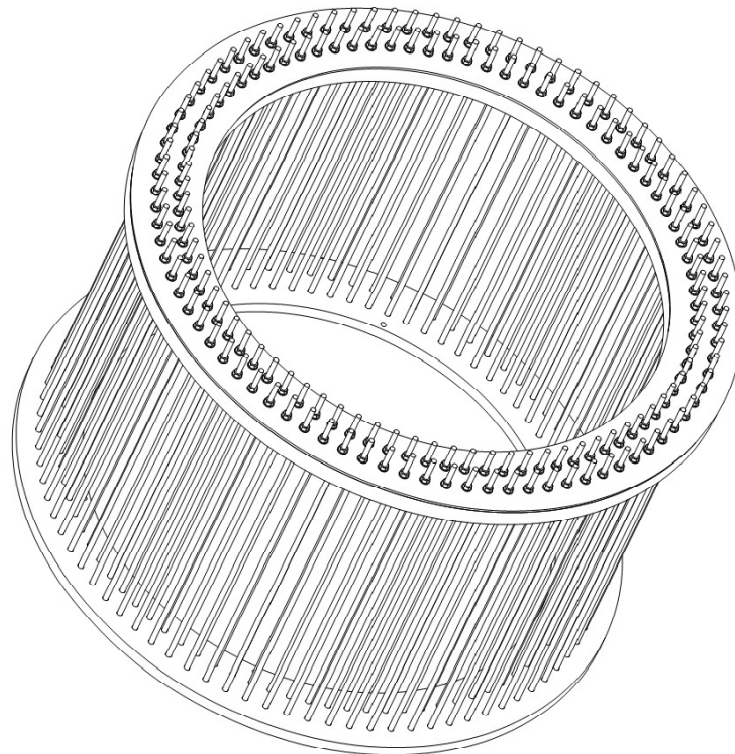# CHALMERS

Numerical Analysis of Wind Power Plant Foundations

Master of Science Thesis in the Master's Programme Structural Engineering and Building Technology

ARVID LINDGREN
OSCAR PAGROTSKY

Department of Civil and Environmental Engineering
Division of Structural Engineering
Concrete Structures
CHALMERS UNIVERSITY OF TECHNOLOGY
Göteborg, Sweden 2014
Master's Thesis 2014:83

Numerical Analysis of Wind Power Plant Foundations

Master of Science Thesis in the Master's Programme Structural Engineering and Building Technology

ARVID LINDGREN

OSCAR PAGROTSKY

Numerical Analysis of Wind Power Plant Foundations
Master of Science Thesis in the Master's Programme Structural Engineering and Building Technology
ARVID LINDGREN
OSCAR PAGROTSKY

Department of Civil and Environmental Engineering
Division of Structural Engineering
Concrete Structures
Chalmers University of Technology
SE-412 96 Göteborg
Sweden
Telephone: + 46 (0)31-772 1000

Cover:
The anchorage cage which is cast into the foundation, securing the tower in place. Edited from (Vestas Wind Systems A/S, 2010).

Numerical Analysis of Wind Power Plant Foundations

Master of Science Thesis in the Master's Programme Structural Engineering and Building Technology

ARVID LINDGREN

OSCAR PAGROTSKY

Department of Civil and Environmental Engineering

Division of Structural Engineering

Concrete Structures

Chalmers University of Technology

ABSTRACT

The extended use of renewable energy has led to a dramatic increase in the development and production of wind power plants. With development of larger plants, foundation sizes have also increased. As foundation size has increased, so has the need for better tower-foundation connections. A new solution is the use of an anchorage bolt cage embedded in the foundation, securing the tower to the foundation by a post-tensioning connection.

The purpose of this thesis was to assess the anchorage cage-tower connection. By a series of finite element models, focusing on the area around the connection as well as the effects on the post-tensioning force during extreme loading, the anchorage cage connection was studied from a local and global perspective. The long-term influence of creep and steel relaxation on the local level was also implemented.

Because of the complexity of the structure, with several different types of concrete as well as post-tensioned bolts going through the entire structure, the modeling was done in steps. By a stepwise modeling process each complexity was isolated and dealt with separately, while evaluating the suitability to use advanced finite element modeling as a design and analysis tool for wind power plant foundations.

By combining the models of different levels, results were drawn locally and globally, together representing the anchorage cage-tower connection. The combined evaluation indicates that some multiaxially compressed areas exceed unconfined design strength of the concrete. The local tensile forces acting on the bolt is greater than the post-tensioning force, while still being well below design yield strength of the bolt. The time consuming modeling and computing, combined with the specific results produced in advanced 3D solid finite element analysis were concluded a very able evaluation tool but not as fitting to use as a designing tool for wind power plant foundations.

Key words: wind power plant foundation, Brigade/Plus, Abaqus, anchorage cage, contact conditions, finite element, solid element.

Numerisk analys av vindkraftverksfundament
Examensarbete inom Structural Engineering and Building Technology
ARVID LINDGREN, OSCAR PAGROTSKY
Institutionen för bygg- och miljöteknik
Avdelningen för Konstruktionsteknik
Betongbyggnad
Chalmers tekniska högskola

SAMMANFATTNING

Den ökade användningen av förnyelsebar energi har lett till en dramatisk utveckling och produktion av vindkraftverk. Parallellt med utvecklingen av större anläggningar har även storleken på fundamenten ökat. Då storleken på fundament har ökat, så har även behovet av bättre torn-fundamentanslutningar ökat. En ny lösning är att använda en ankarbur, ingjutet i fundamentet, för att säkra tornet till fundamentet.

Syftet med denna tes var att bedöma torn-fundamentanslutningen. Genom en serie av finita element modeller, med fokus på det lokala området runt anslutningen samt effekterna på efterspännkraften under extrem belastning. Ankarbursanslutningen studerades ur ett lokalt och globalt perspektiv. Den långsiktiga inverkan av krypning och stålrelaxation på lokal nivå har likaså studerats.

På grund av komplexiteten i konstruktionen, med flera olika betongtyper samt efterspända bultar som går genom hela strukturen, genomfördes modelleringen i steg. Genom en stegvis modelleringsprocess var varje komplexitet isolerad och behandlad separat, samtidigt möjliggjordes en utvärdering av avancerad finitelementanalys som metod för att utvärdera och utforma vindkraftverksfundament.

Genom att kombinera modellerna på olika nivå, kunde resultat nås på lokalt och global nivå, vilket gav en total representation av ankarburen och tornkopplingen. Utvärderingen av resultaten visar att en del områden under biaxiell last överträffar det tillåtna dimensionerande värdet av betongens hållfasthet. De dragkrafter som verkar i bulten är högre än inspänningskraften, samtidigt som de var klart under både bultens flytgräns och brottgräns. Modellerandet och analysen i FE-programvaran är mycket tidskrävande, men med de specifika och precisa resultaten drogs slutsatsen att finita element är ett bra utvärderingsverktyg men inte optimalt för utformning av vindkraftverksfundament.

Nyckelord: Vindkraftverksfundament, finitelementanalys, ankarbur, kontaktvillkor.

Contents

Preface

After completing this project it is clear that it would not have reached its final stage without a pair of key individuals; us.

With that said some specific recognition are in order:

To our supervisor Rasmus Rempling at Chalmers, for valuable input and keeping us on track. Karl Lundstedt at Skanska for the idea of the project, tutoring and inputs throughout the process. Rikard Nagy at Skanska for weekly correspondence and help regarding everything from calculations to software setup. Helena Burstrand Knutsson for supreme patience in early stages and oversight at the office. To Johan Skalin for inviting and showing us his ongoing project. To Björn Engström at Chalmers for inputs and guide lines. Last but not least, our opponent, Fredrik Davidsson, for all your valuable thoughts.

Arvid Lindgren and Oscar Pagrotsky
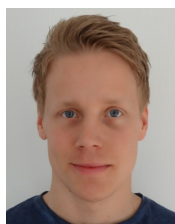
Göteborg, June 2014

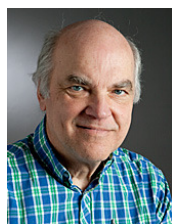
Arvid Lindgren

Oscar Pagrotsky

Rikard Nagy

Fredrik Davidsson

Björn Engström

Karl Lundstedt

Helena Burstrand Knutsson


Rasmus Rempling

"Voiceless it cries, Wingless it flutters, Toothless it bites, Mouthless it mutters"

- J.R.R Tolkien

1   Introduction

During recent years a rising demand for renewable energy sources have lead to a rapid increase in production and development of wind power plants (WPP) all over the world; only in Sweden the installed effect from wind power plants have increased tenfold over the last ten years (Swedish Energy Agency, 2013). Simultaneously have the rotor blade length, hub size and tower height increased rapidly in order to maximize the output and effect of each power plant. As a result, the foundations are also becoming bigger and bigger and thus more expensive (Veljkovic, 2014). By optimizing the different systems, costs and sizes can be cut in favour of more efficient systems.
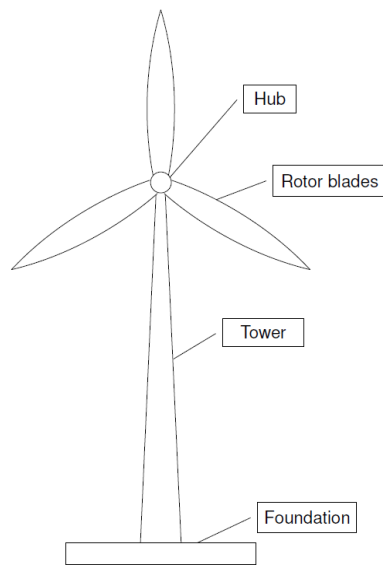
Figure 1:1 Different parts of a wind power plant, adopted from (Göransson & Nordenmark, 2011).

As suggested by Göransson and Nordenmark (2011), the compressive zone under the tower and the tower-foundation connections are areas of interest for optimization of wind power plant foundations. This study thoroughly dissected and studied these areas with the aim of being an aid in future design.

The last years' transition from insert rings, a large steel tube, to a more effective anchorage cage has solved some earlier problems in design. This new solution still leaves some questions to be answered; local extreme pressures under the ring and loss in tension in the bolts due to long term effects are yet to be examined. Opinions differ in how to treat these with regard to load cases and partial factors.

International committees are at the present trying to find an appropriate way of dimensioning loads from the different codes and regulations, to see which cases actually would be decisive in design.

1.1 Aims and objectives

The performance of the anchorage cage-tower connection was evaluated by studying the following areas:

- Analyze local pressures in the concrete under the tower flange, with focus on material strength in the grout, plinth and plinth-base contact zone, described in Figure 1:2.
- Study the effect of loss in tension of the post-tensioned anchor bolts during extreme loading.
- Study the long term effects on the post-tensioning force.
- Combining local and global analyses to identify areas of interest for structural design.

Also, an evaluation of the suitability to use advanced finite element modelling (FEM) as an analysis and design tool of wind power plant foundations, was preformed.
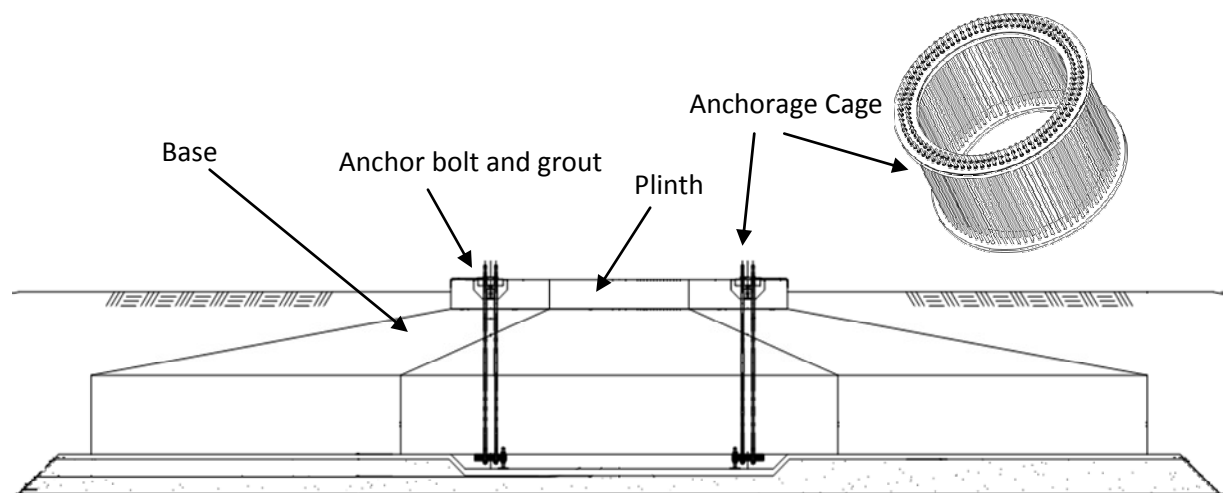

Figure 1:2 Picture of foundation slab, describing the above mentioned areas.

1.2 Method

The project started with a literature study regarding fatigue of reinforced concrete and the production process as well as design of wind power plants.

The aims and objectives were studied through the following finite element models, all with their specific purposes.

- **Simple 2D plate model**.
    - o This model was used for assessing the equilibrium conditions and reaction forces, later used as a reference for the more complex models. The model was validated by calculations done in the reference project.
- **Bolt-concrete models**.
    - o These models were used for closer investigation of the contact conditions used between the steel and the concrete, as well as the different concrete classes.

o The models were validated through hand calculations of force and strain equilibrium.
- **Bolt-pair model,** a cut out of maximum loaded section of the anchorage cage.
    o This model was a local model with the dimensions and loads from the reference object.
    o This model was used to study the local effects around the anchorage cage-tower connection, as well as long term effects and the loss in tension of the bolts.
    o The model was validatied through hand calculations of force and strain equilibrium.
- **Section model,** a thin cut out of the maximum loaded section of the entire length of the foundation.
    o This model was used to study the global force pattern in the maximum loaded section and its influence on the anchorage cage-tower connection.
    o The model was validated by comparison with the earlier plate model, with specific focus on soil pressure.

Lastly the results from the models were compiled and analyzed. Conclusions drawn with regard to the aims and objectives followed.

Reference project

The models were validated through the reference object *Örken*, a wind power plant park in Halland, Sweden, for which the foundation design with appropriate calculations and input and output data are available.

The turbine used in the project is a Vestas 94 meter high and 3 MW power plant, the input loads were given by Vestas. The foundation used at Örken is an octagonal gravity foundation on natural soil.

1.3 Limitations

The first and most important limitation of this study is that the dimensions and loads are all based on the reference project, *Örken*. The detail for fastening the power plant in the foundation looks principally the same in almost all foundations regardless of fasteners/reinforcement layout and design.

The geotechnical parameters in this study were simplified to the point where the soil was modelled as simple non-linear springs, only acting in compression and stiffness based on the reference project.

The software used were Brigade/Plus and FEM-design 13. Brigade/Plus mainly because of previous experience with the ABAQUS based program and since the support and development center is based in Lund, close to the Malmö office of Skanska. FEM-design 13 because of its use in the reference project.

2 Background

2.1 Brief historic background on wind power

The electrical power plant saw its first light in the late 19th century, and was continuously developed during the first half of the 20th century. Even though numerous models where developed and tested, none proved to be profitable and therefore never had a break trough.

This all changed in the late 1970´s when the oil crisis hit. All of a sudden oil prices increased dramatically, giving the wind power industry a well needed push. With the help of government funded research the wind power plant market grew, first with small scale systems, later bigger and bigger systems as displayed in Figure 2:1 (Gasch & Twele, 2012).
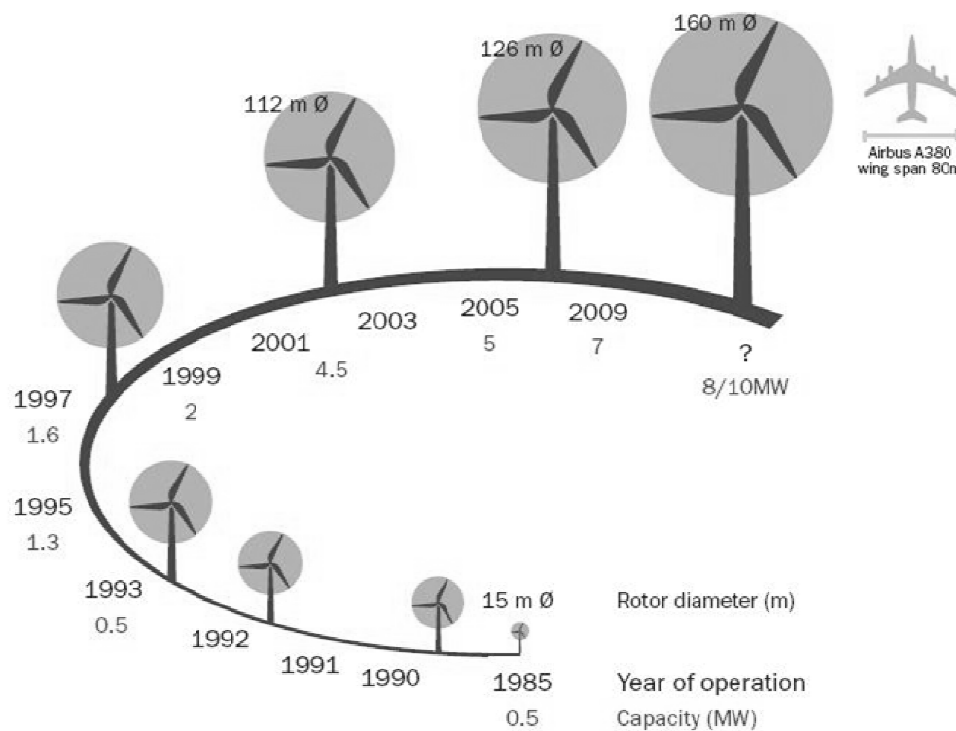

Figure 2:1 Evolution of wind power, from (European Commission, 2013).

2.2 Foundations today

Wind power plant foundations are normally divided into offshore and onshore structures; these are not as different as they appear. Both are commonly built with reinforced concrete and placed on the ground. Some other types exist, like floating offshore foundations and onshore cable stabilized towers, but these are not common.
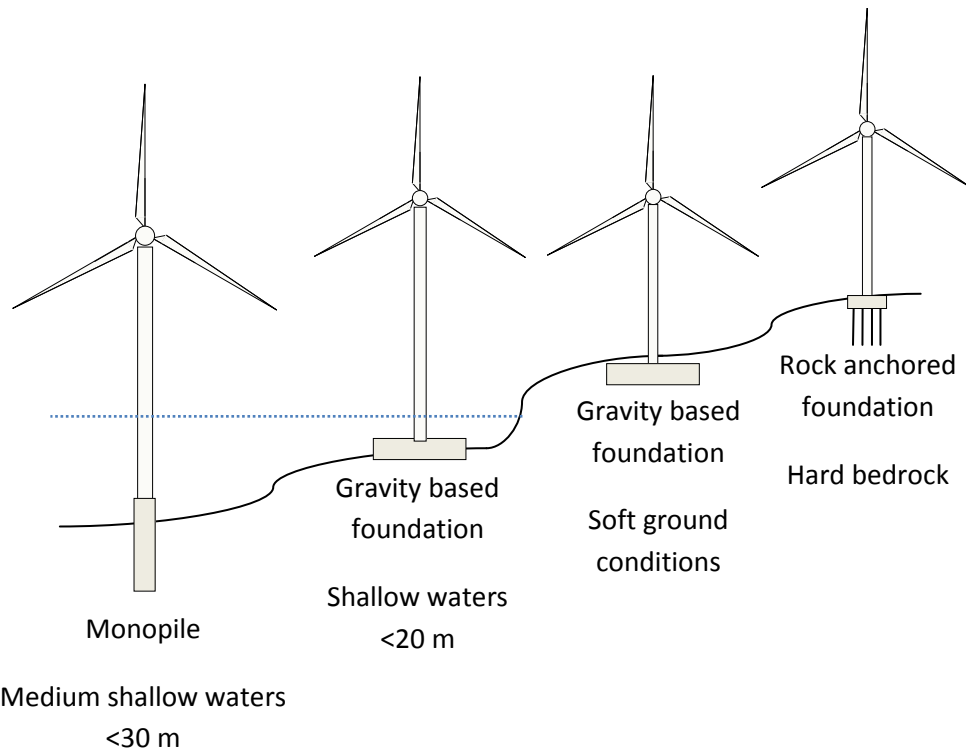
Figure 2:2 Common types of foundations.

The foundations most commonly used offshore are monopile and gravity based foundations. The gravity based type is basically the same as the most common onshore foundation, which also is a gravity based foundation. (Gasch & Twele, 2012)

Likewise, the onshore foundations are also divided into different types of foundations, gravity based and rock anchored slab foundations. The rock anchored type is normally of a smaller size, since the anchoring increases the overturning capacity of the foundation.

The gravity based slabs are either flat on the ground or on a pile reinforced ground. These piles could be connected to the slab itself, thus giving an increased overturning capacity.

While the tower-foundation fastening only varies with tower model, the ground contact area of the slab varies greatly in between the different slab types. This is since the overturning capacity varies greatly in between the different slab types; a non-anchored slab needs a larger ground contact area to achieve the same overturning capacity as an anchored slab.

The different types are generally chosen on the basis of geotechnical conditions and therefore economic reasons. A soft soil would require a large foundation area to counteract the overturning, in such a case it might be more appropriate to utilize something anchored in the bedrock.

Sizes and shapes of slab foundations vary, mainly in between rectangular and octagonal shapes. In short, a rectangular shape is easier to design and construct, while an octagonal shape uses less material (Burton, 2011).

2.3   Foundation design

There are four main loads acting on the foundation: overturning moment, horizontal force, vertical force and torsion, as illustrated in Figure 2:3. The overturning moment is mainly generated from the drag of the rotor blades acting high above the foundation, but also includes 2nd order effects as well as the added moment from unintended inclination of the structure. The horizontal push on the rotor is transferred as a sliding force on the slab.

Vertical forces acting on the foundation are primarily from the weight of the blades, hub and tower. These forces can act as a favorable stabilizing load, when designing for the moment and must in that case be reduced with proper partial safety factors.

A rotational moment around the tower's axis also occurs, but is small in comparison to the other forces.
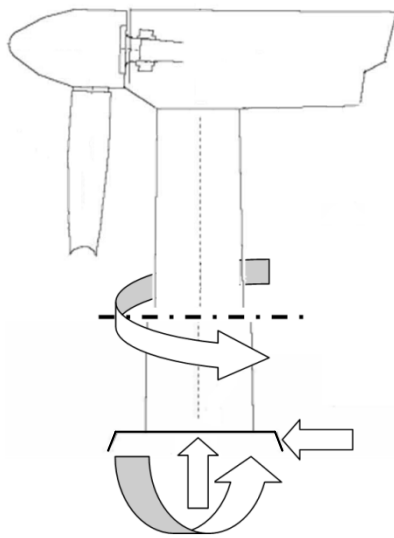

Figure 2:3 Reaction forces in the foundation slab, the overturning moment, horizontal forces, vertical force and torsion generated by the non-symmetric rotor configuration. Edited from (Vestas Wind Systems A/S, 2010).

To withstand the loads on the foundation slab, the design has to be fit to handle all types of loads and load combinations.

To counteract the overturning of the WPP structure; the foundation slab transfer the load to the soil, keeping ground pressure low by designing with a sufficiently large contact area.

The horizontal force is in general small with regard to the weight of the tower and slab, the horizontal sliding resistance is made sufficient by the weight of the components and friction against the bottom of the foundation as well as the height of the rim.
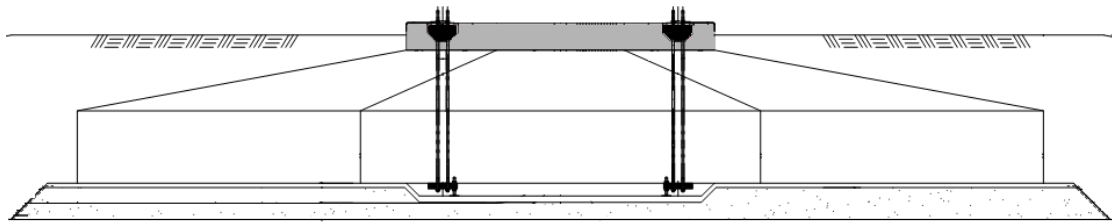
Figure 2:4 Cross section of an octagonal slab, with the ground surface shown by the hatched lines. Grout shown in black and the plinth in grey.

The vertical force from the tower and nacelle counteracts the overturning forces. However, in the project Örken, the vertical force is only about 1:20th of the overturning forces, thereby not affecting design as much as the dead weight of the foundation.

To ensure the anchorage and to distribute the force from the tower, an anchorage cage is cast into the foundation. This anchorage cage, illustrated in Figure 2:5, consists of numerous high strength steel bolts. In the bottom of the cage, the bolts are anchored to a steel ring and in the top, to the tower bottom. The top ring, i.e. the tower bottom, is fastened by post-tensioning of the bolts. To ensure that the stresses are distributed to the steel rings, the bolts are placed in PE-tubes, ensuring a frictionless interaction with the surrounding concrete.
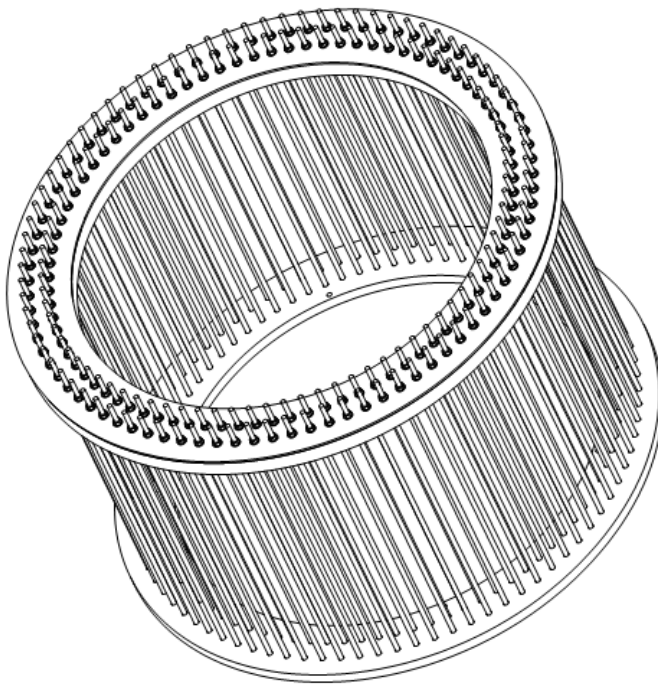

Figure 2:5 Sketch of the anchorage ring, with the connecting bolts.

The post-tensioning and moment leads to extreme pressures, especially just below the tower flange. To handle these extreme forces, high strength grouting, often above strenght classes of 100 MPa in characteristic compressive strength (PAGEL Spezial-Beton, 2013) is used. This high strength concrete's main purpose is to dissapate the extreme pressures down to the concrete plinth.
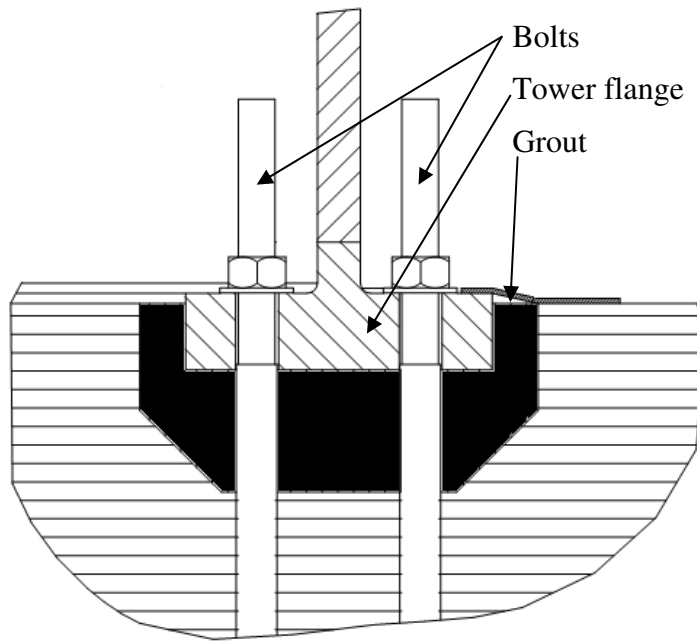
Figure 2:6 Cross section of the grout (black) and the anchorage ring connection.

The plinth, shown in Figure 2:7, is the second part transferring the high pressures from the tower/tensioned bolts to the entire slab.
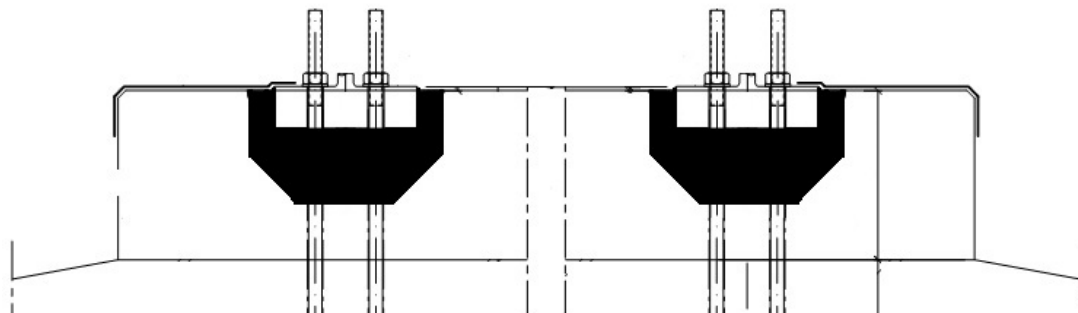
Figure 2:7 Cross section of the plinth, with the grouting shown as black areas.

In the plinth, a weaker concrete class is used, often C45/55, since the stresses are not as concentrated as around the tower flange. The plinth rests on the foundation base that is cast in a regular type concrete C32/40. The bolts shown in the pictures above and below are cast into the slab and post-tensioned from the top, thus using the full height and width of the slab, as well as ensuring a firm anchoring.
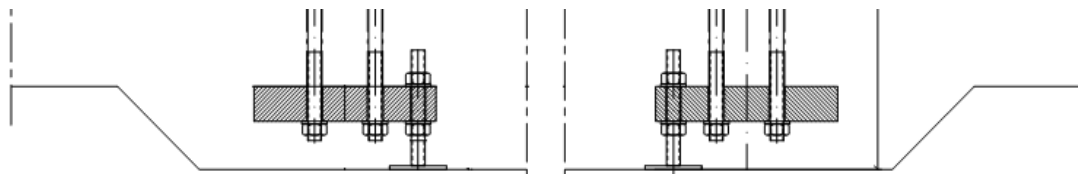
Figure 2:8 Fastening of the anchorage ring inside the bottom of the slab.

The force distribution through the different components and materials in combination with long term effects, such as shrinkage, creep and stress-strain relaxation, is hard to predict. Without an accurate stress distribution prediction, fatigue is difficult to design for.
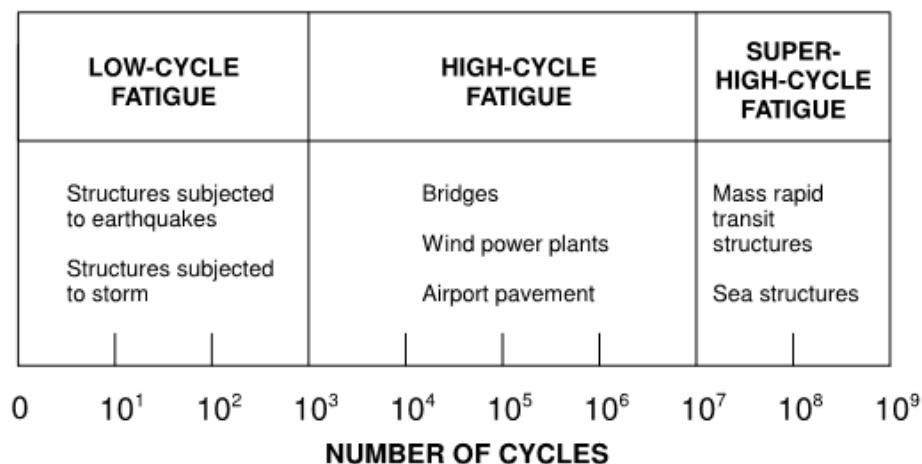
2.4 Fatigue

Wind power plants are not only loaded with static loads during their designed life. Because of the rotors and turbulence vibrations are transferred to the tower and down to the foundation, these vibrations fatigue may cause fatigue cracks to develop.

2.4.1 Fatigue in general

During cyclic loading, structural systems or structural components can fail before the ultimate static stress capacity is reached. This phenomenon is known as fatigue, and it is influenced by factors ranging from the geometry of the loaded component to the amplitude of the load (Dowling, 2013). This leads to certain design scenarios where the fatigue strength, not the ultimate static strength, is the governing factor.

As fatigue is a result of cyclic loading it is generally divided into different categories dependent on how many load cycles a component experiences during its designed life span. Structures subjected to traffic loads or vibrations due to wind is normally considered affected by high-cycle fatigue, while an earthquake does not induce the same amount of cycles i.e. low-cycle fatigue.

Figure 2:9 General way of classifying fatigue with regard to load cycles, from (Göransson & Nordenmark, 2011).

To describe and estimate a component's fatigue life with regard to load amplitude and cycles, a stress to number of cycles curve (S-N curve) or a Wöhler curve is used. It is a logarithmic diagram where cycles to stress amplitude is plotted. Usually if stress amplitude is known it is possible to derive how many cycles the design life would be or if the cycle count is known, maximum amplitude can be derived in the same reversed manner.

The curves are based on tests and the following design curves are drawn with proper safety factors (Dowling, 2013).
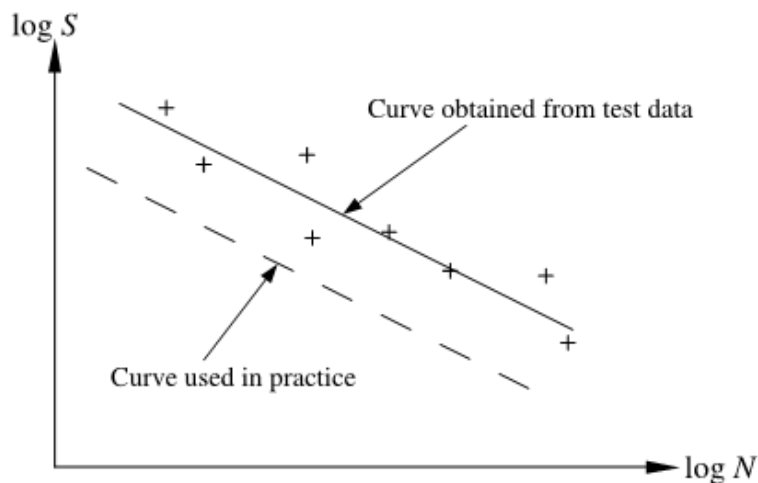
Figure 2:10 Conceptual Wöhler curve, from (Göransson & Nordenmark, 2011).

The S-N curves are material and detail dependent; when two materials act together like a composite, the S-N curve is not as straight forward to use (Dowling, 2013).

Some materials, for example steel, have an apparent lower bound stress limit for which loading cycles can be repeated infinitely without a fatigue failure occurring. Concrete on the other hand does not, the difference in the two being that steel is a strain hardening material (strength increases at large strains) and concrete being a strain softening material (strength decreases at large strains).

When explaining fatigue, the chain of events is often divided into three different parts: initiation, propagation and finally failure. Here there is a big difference in the behavior of homogenous materials like steel; and composite materials like concrete/reinforced concrete (Thun, 2006).

2.4.2   Steel

Cyclically loaded steel fatigues in two phases; the microscopic initiation phase and the macroscopic propagation phase.

Initiation phase is marked by microscopic cracks starting at the surface of the steel as a shear slip between crystal planes. When loaded cyclically, these cracks grow larger and larger, eventually cracking entire grains. When these micro cracks propagate through several metal grains, they create a larger macro crack.

Propagation phase is defined by macroscopic cracks, which propagates for each load cycle that the component experiences. When the crack finally reaches the point of failure, the specimen suddenly fractures in a brittle manner (Dowling, 2013).

2.4.3   Concrete

Concrete subjected to high cycle loading, like WPP foundations, normally suffers fatigue damage from crushing in compression and crack propagation in tension. Permanent fatigue damage occurs from about 70% of peak load (Shah & Mu, 2005).
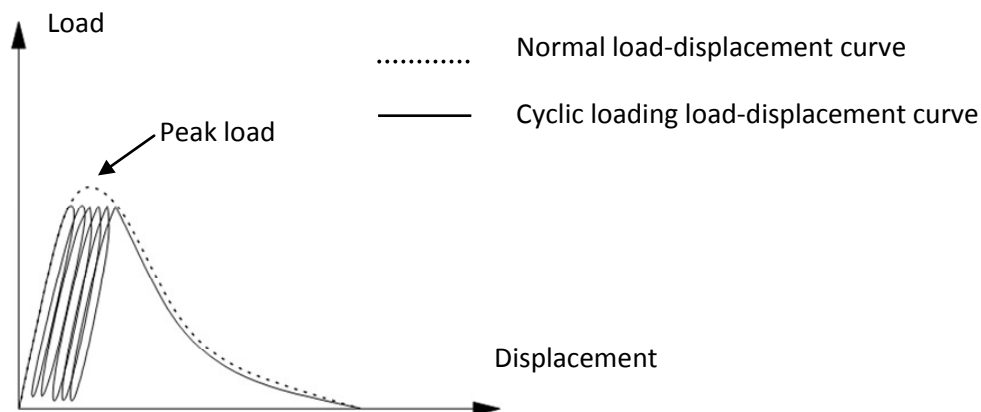
Figure 2:11 Stress strain curve of concrete. Each loading cycle results in a permanent deformation, from (Rempling, 2009).

Contrary to steel, concrete does not have a crack initiation phase, since the concrete cracks on a microscopic scale during its hardening process; due to internal settlements, plastic shrinkage and temperature development. These small cracks are evenly spread across the material and therefore there are always cracks present (Engström, 2011).

The propagation phase is defined by the joining of micro cracks into larger macro cracks. These macro cracks propagate faster than the micro cracks and are the deciding factor for the remaining fatigue life of a concrete component (Olsson & Pettersson, 2010).

While concrete normally is seen as a homogenous material, in fact it is not. On an up close level, so called meso level, the concrete consists of different areas with different stiffness; normally aggregate, cement paste and an interaction zone. This difference in stiffness makes it hard to estimate where macro cracks will propagate and thus where fatigue problems will occur.

2.4.4   Reinforced concrete

When combining the stiffer steel with less stiff concrete, the system becomes much more complex. As soon as the concrete cracks and the reinforcement is loaded, the force pattern changes; the stress increases in the stiff reinforcement and decreases in the less stiff concrete (Engström, 2011). This can lead to intricate force patterns which in turn can be difficult to predict and calculate in detail.

The interaction zone in between the reinforcement and the concrete can be a crucial area; if the reinforcement is heavily loaded the concrete around the bars can fail and there after lead to a bond slip failure.

2.5   Uniaxial, biaxial and multiaxial loading of concrete

2.5.1   Uniaxial loading and strength

To determine compressive strength class of concrete, according to the European Standard, a concrete specimen is uniaxially loaded until failure and thus the class is determined, as shown in Figure 2:12.

However, there are two types of test specimen; a cylinder measuring 300mm in height and 150mm in diameter and a cube with the side of 150mm. As a general rule the cubic test strength is 1.2 times higher than the cylindrical which is due to the state of stress in the respective specimens.

The cube has a larger surface area with regard to total volume in contact with the testing rig compared to the cylinder test. This has a positive influence with regard to the compressive strength, since the boundaries will have a retaining force created from the preventing of volumetric strain. This influences the entire cube; while in the cylinder, because of its height, the failure of the concrete is largely affected by the lateral tensile stresses owing to the Poisson effect (Domone & Illston, 2010), as described in Figure 2:12.
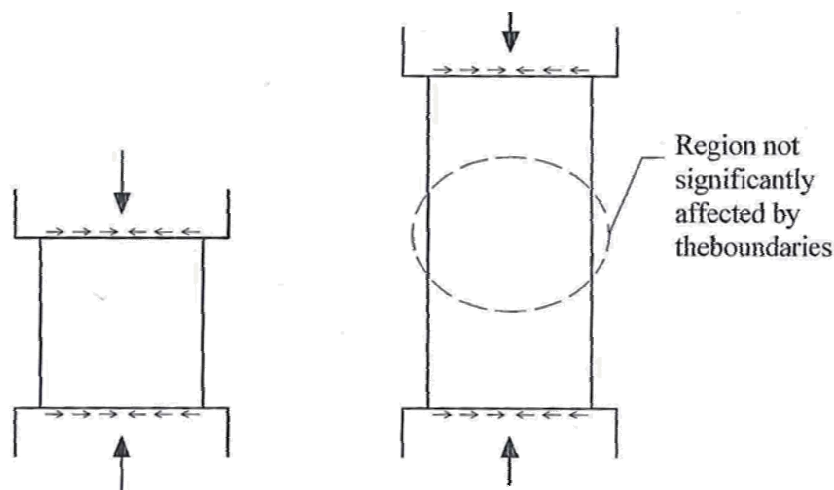

Figure 2:12 Influence of boundary conditions in compressive stress test, from (Engström, 2011).

2.5.2 Biaxial loading and strength

When a uniaxially loaded specimen is being contained with another perpendicular load it is called biaxial loading. In biaxial tests it has been shown that concrete under dual compressive stress increase its resilience. This case is opposite when it comes to tensile-compressive biaxial loading, resulting in a lower compressive stress resistance of the concrete (Engström, 2011).

As the graph in Figure 2:13 illustrates in the first quadrant, a combination of biaxial compressive stresses increases the strength, compared to the uniaxially loaded concrete. In the same manner, a tension-compression combination, as quadrant two and four, reduces the strength of the concrete.
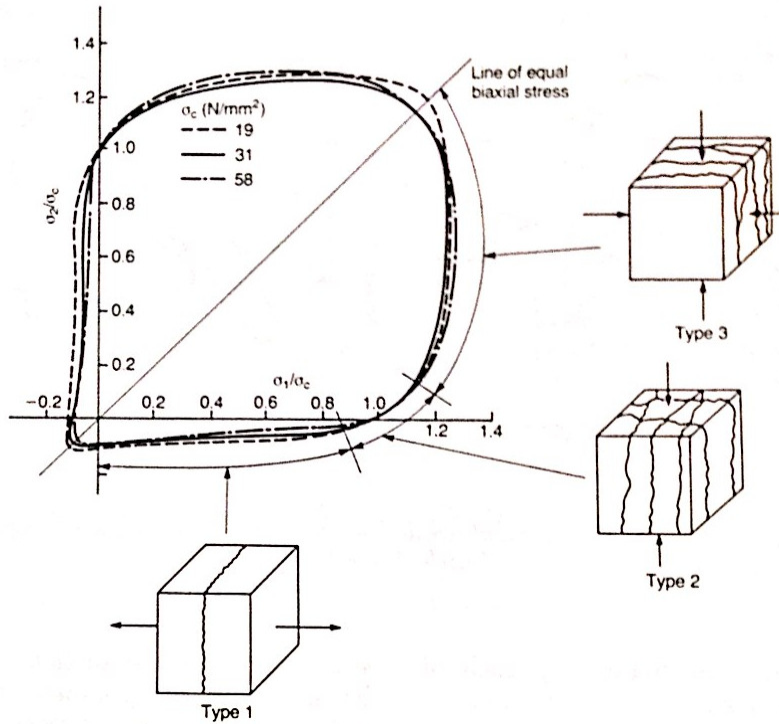
Figure 2:13 Biaxial strength plotted against the relation with the containing force and the characteristic uniaxial strength, where type 1, 2 and 3 are representing the different crack patterns at failure for different loading situations. Note type 3; when compressed in both directions the sample cracks outwards in the unconfined direction, edited from (Domone & Illston, 2010).

2.5.3   Triaxial compression

In states where concrete is stressed in all three principal directions its compressive strength is greatly increased (Engström, 2011). Since the tensile stresses occurring are compensated by the compression, no tensile stresses occur and therefore no tensile cracks appear (Domone & Illston, 2010). The failure in such a specimen is in pure compressive crushing.

In Eurocode it is handled as an increase in strength based on the utilization degree with regard to characteristic compressive strength.

$$f_{ck,c} = f_{ck} * (1,0 + 5,0\sigma_2/f_{ck}) \qquad \text{for} \qquad \sigma_2 \leq 0,05 f_{ck} \qquad (2.1)$$

$$f_{ck,c} = f_{ck} * (1,125 + 2,5\sigma_2/f_{ck}) \qquad \text{for} \qquad \sigma_2 > 0,05 f_{ck} \qquad (2.2)$$

$f_{ck,c}$: *Characteristic confined compressive strength.*

f_{ck} : *Characteristic compressive strength.*

In theory, the compressive strength could increase with 262.5%. This is during a loading case where the two retaining pressures are of equal magnitude, see Figure 2:14.
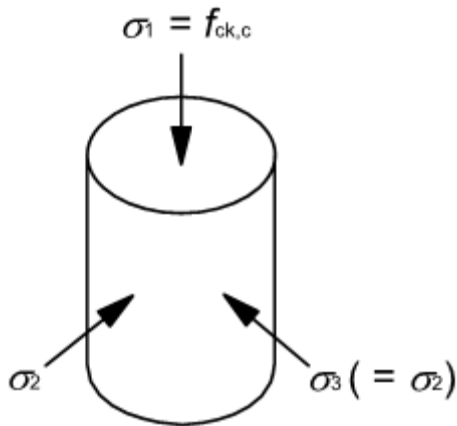
Figure 2:14 Multiaxial stress, from (European Comittiee for Standardization, 2008).

2.6 Key phrases and words

As this study relied heavily on a set of finite element (FE) models, some key phrases are important for the understanding of coming chapters.

- *Rigid body motion (RBM)* – A rigid body that has an unhindered motion, usually occurs in FE analysis when a rigid body does not have appropriate boundary conditions.
- *Step* – In finite element modeling, it is possible to combine several analyses in one computation, each analysis being a *step*. In this manner, it is possible to base one analysis on results from a previous one, as well as to change boundary conditions and variable inputs in the same computation.
- *Contact condition* – Mathematically describing how two surfaces behave with regard to one another. Crucial for the model since this determines how stress and deformation transfers between different surfaces, e.g. how the bolt interacts with the surrounding concrete or how the steel ring interacts with the grout.
  - *Tangential interaction*
    - *Rough* – Is when the two surfaces do not slide over each other, shear loads will be transferred over the surface.
    - *Frictionless* – when sliding is not prevented, must in most cases be supplemented with additional boundary conditions to prevent rigid body motion.
  - *Normal interaction*
    - *Hard* – the physical representation of reality, when two objects or surfaces are in contact they transfer load. Can be combined with a so called penalty condition, wherein the forces transfer over a distance before they are in contact. The penalty condition is not a true representation of reality, but can be a faster way to get convergence.

- *Surface-to-surface and surface-to-node contact discretization.*
  - *Surface-to-surface* – Each slave node will affect a region with an averaged contact condition, each region will in turn overlap other such regions, resulting in each contact affecting multiple nodes. This type of discretization is less prone to have stress spikes in nodes and tends to provide more accurate results. The direction of the contact will be based on the average normal of the slave surface. This can be problematic when designing sharp, pointy objects.
  - *Surface-to-node* – Each node has its own contact condition, resulting in the possibility of penetration of individual nodes. The direction of the contact is based on the normal of the master surface.
- *Master and slave surface*
  - *Master* – Normally the larger of the interacting surfaces. If there is a great difference in stiffness of the interacting structures the surface of the stiffer structure should be master. The master surface can to some extent penetrate the slave surface.
  - *Slave* –The opposite of the master surface. Should be more densely meshed than the master surface, since it can be penetrated by the master surface. However, this is a rather small problem on surface-to-surface interaction, compared to node-to-surface interaction where single master nodes are prone to penetrate the slave surface.(Dassault Systèmes, 2012).

3 Local Pressures Under the Tower Flange

To answer the first objective, to analyse local pressures under the tower flange, with focus on the grout and plinth, a model representing these local areas of the reference foundation was needed. The bolt pair section, shown in Figure 3:1 was decided to sufficiently represent the local stresses and forces in these areas. The model was analyzed at the maximum compressed section of the flange, naturally affecting the areas the most.
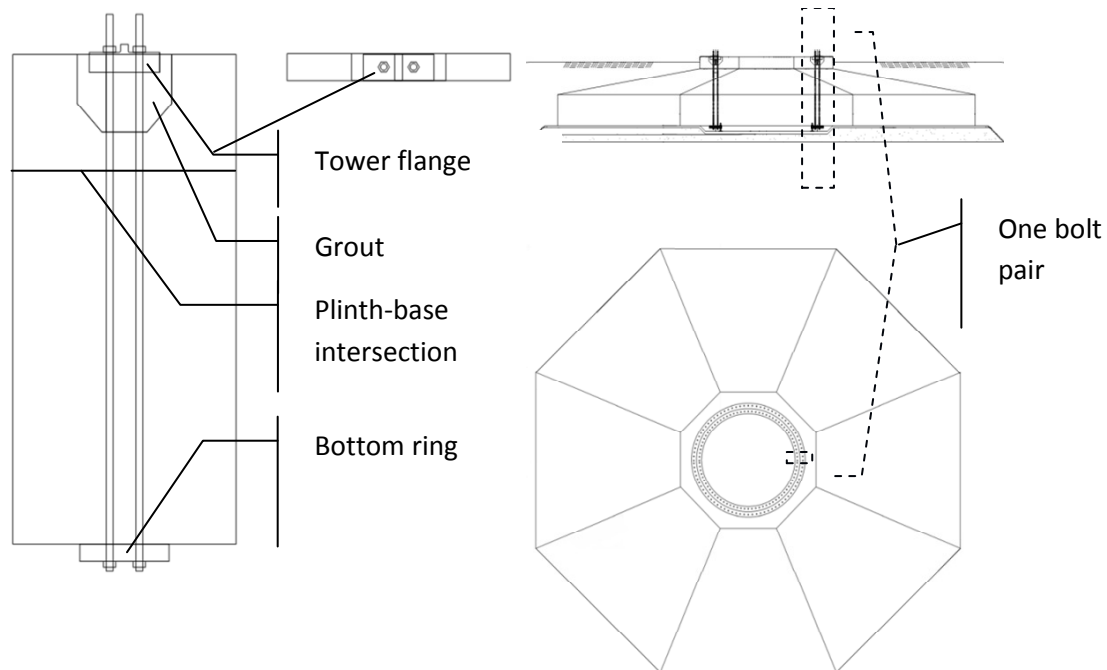

Figure 3:1 Section of model and its location in the reference foundation.

Due to the complexity of the foundation design and the characteristics of the section, several modelling challenges were expected. The challenges recognized were mainly material interaction properties and post-tensioning of the bolts. These were isolated and modelled separately, thus simplifying the solution of each challenge. Four models were made to solve these challenges, refining the model in each step, followed by the more complicated bolt-pair model representing the reference foundation. The four isolated models were:

- *Concrete-steel contact condition,* crudely representing the tower flange.
- *Concrete-concrete contact conditions*, representing the multiple concrete classes.
- *Bolt-concrete frictionless interaction,* simulating the plastic tubes around the bolts.
- *Post-tensioning of the bolt,* modelling the post-tensioning of each bolt realistically.

3.1 Concrete-steel interaction model

The contact condition between the plate and the concrete was not as complicated as initially believed. It was easily done with a normal and tangential property, where the

tangential handles the shear interaction of the parts and the normal translates the forces from the steel plate to the concrete column, in the normal direction.

To ensure functioning models, different loads were applied while visually examining the results and comparing the stresses in different sections with hand calculations. The forces applied were: an even pressure over the whole plate, pressure over a small cylindrical area in the middle of the plate and a local pressure, dependent on displacement of the plate. The model is described schematically in Figure 3:2.
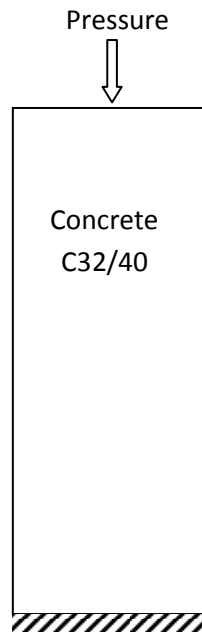
Figure 3:2 A sketch of the first column model with an arbitrary pressure and a locked bottom surface.

The model was created as a column with a locked bottom surface and the pressure applied was arbitrary. The results were validated through deformation calculations based on Hooke's law and linear elastic analysis.

3.2 Concrete-concrete interaction model

This model was an enhancement of the previous concrete-steel model, with a section of stiffer concrete near the steel plate.

Two methods of modeling multiple concrete classes were tested. Firstly a model with multiple parts of different concrete classes, connected with contact conditions, similar to the steel plate. Secondly a single part model, with the different concrete classes integrated into one part, basically one part with a stiff and a weak region. Both methods where able to represent a column with two concrete classes, cast together, in a satisfactory manner. The one part model was slightly faster to model, and thus favorable. Figure 3:3 shows the schematic model of the concrete to concrete interaction test (with the steel plate still in its place) to the left, and the resulting contour plot to the right.
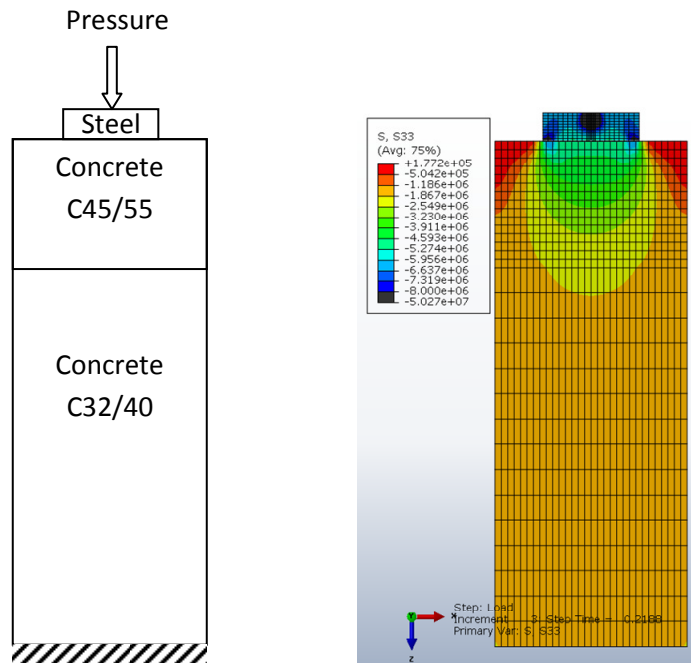
Figure 3:3 Schematic picture of the model to the left. Stresses through the concrete-concrete-steel column model to the right.

This model also had a locked bottom surface and arbitrary pressures applied. It was validated with similar calculations as in the case in Chapter 3.1.

3.3 Bolt-column frictionless interaction model

This model was made to understand how to model the bolts frictionless interaction through the concrete and steel.

As seen in Figure 3:4, the model consisted of a concrete column with steel plates on both sides, with a hole through the center. The bolt was placed in this hole and fastened with nuts in both ends. The bolt was given a frictionless contact condition to represent the plastic tubing preventing contact with the concrete. The nuts, being in direct contact with the steel plate, was given the same hard normal conditions as the plate in Chapter 3.1, transferring all normal forces.
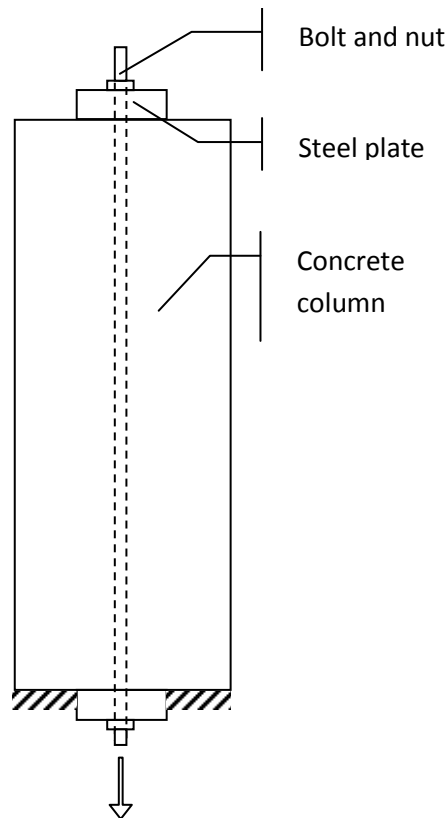
Figure 3:4 Sketch of the bolt-column model.

To test the frictionless contact condition, a tensile force was applied on one side of the bolt, represented by the arrow in Figure 3:4, while locking the bottom concrete surfaces from movement in all directions. Equilibrium comparison between the stresses under the nut on the opposite side from the applied force to the applied force, showed no loss in stress, confirming a frictionless interaction.

3.4 Post-tensioning of the bolt

The post-tensioning of the bolt was modeled in the three methods allowable in the software, to test which one was preferable. These were temperature load, bolt load and bolt displacement method.

- The temperature load is dependent on a material temperature shrinkage factor and an applied temperature change from one step to another. This method was hard to calculate precisely, and had to be solved by iteration and worked well after a few iterative steps. This method shrinks the material in all directions, not only in the desired direction, although this hardly influences the results.
- The bolt load applies a load in a determined section of the bolt, it can be applied in one computing step and then kept at the same equivalent deformation through the following steps, symbolizing a post tensioning of the bolt, followed by other loads.
- The bolt displacement is similar to the bolt load. It is applied in the same manner, but instead of a prescribed load, a displacement is applied.

To verify that the post-tensioning techniques were working, they were computed in two steps, one with only the post-tensioning, followed by one with an arbitrary pressure on the steel plates. The arbitrary applied force resulted in a deformation of the plates and the concrete, this deformation led to an equal reduction of force in the bolt.

The deformation based methods was dependent on meshed size making the forces-displacement relationship dependent on mesh structure. As mesh elements consists of non-curved, straight sides, a circular area has to be represented as a polygonal shape. Thus an applied stress, or deformation induced stress, over a polygonal shape will be less than the stress over a circular shape as illustrated in Figure 3:5. However this can be calculated but still is a possible source of errors.
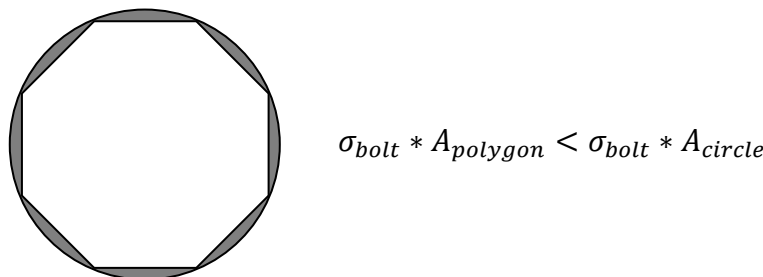
$$\sigma_{bolt} * A_{polygon} < \sigma_{bolt} * A_{circle}$$

Figure 3:5 The difference in area over a polygon contra a circle.

All methods worked, but the bolt load method was preferred since it uses force as input, instead of a deformation. As the reference object uses a prescribed post-tensioning force, not a deformation, the bolt load tool was easier to apply.

3.5 Bolt-pair model

With the expected challenges solved, the bolt-pair model based on the reference object was created. The model was made with a symmetry condition, to cut down on computing time. Also, the boundary condition was more challenging than expected.

3.5.1 Symmetry

Because of the shape of the model, it was possible to create half the model and assigning a symmetry condition that mirrored the forces in the assigned section, resulting in a full model, computed as a half model, as shown in Figure 3:6.

To verify that the symmetry model actually represented a full scale model; both were made. By examining the stresses in the symmetry section, through the bolt, around the plinth and the grout, the models was confirmed perfectly similar. Thus symmetry modelling was thereon used.
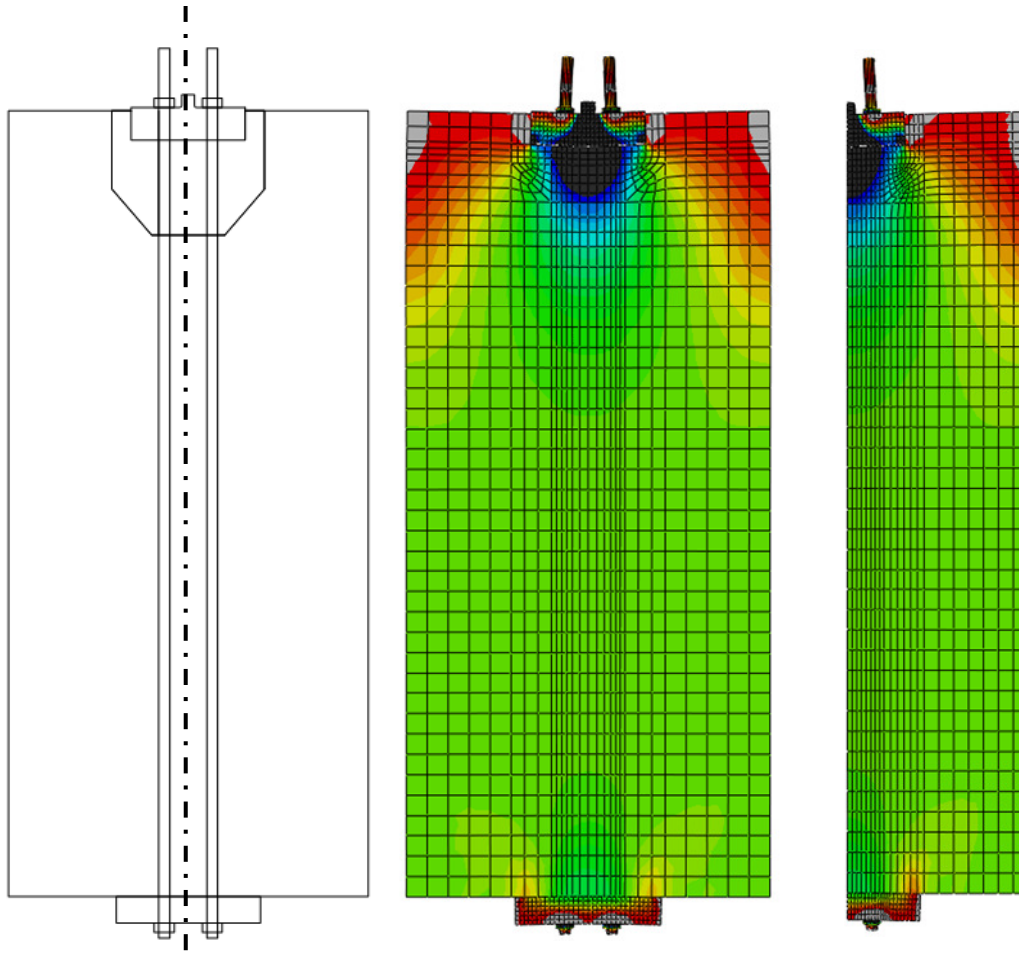
Figure 3:6 From the left; Sketch of the slice model with symmetry line, full model and symmetry model.

3.5.2 Boundary conditions

The boundary conditions of the model were not as straight forward as expected. Three different boundary conditions were tried; locked edge node, springs and locked surface. These were applied to the surface shown in Figure 3:7.
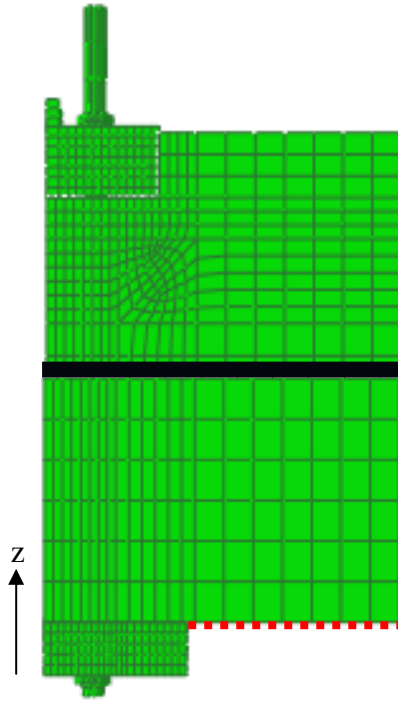
Figure 3:7 A cropped half of the bolt-pair model with a dotted boundary surface.

By locking the surface in the z-direction, it was possible for the model to converge without any singularities. However, this did not represent reality, as this would indicate that the concrete would work as a column and not as an isolated part of a larger system. Nonetheless, the local effects at the grout, plinth and top base are still considered correct with regard to the results needed for this objective.

3.5.3 Loads

The two loads applied in the model are the bolt post-tensioning and the external loads from the tower. The load from the tower is a combination of the tower self weight and the equivalent force from the ULS bending moment. To represent the bending moment as a linear load over tower flange, first order beam theory relating to a thick walled tube was used, described in Equation 3.1 and 3.2. Figure 3:8 illustrates, the bending moment distributed linearly over the whole flange. In this model, the load at the maximum section was used, with correlating partial factors.

$$\sigma_{m\,z}(x) = \frac{M_{ULS}}{I_{tube}} * x \tag{3.1}$$

$$I_{tube} = \frac{\pi}{4}(r_2^2 - r_1^2) \tag{3.2}$$

M_{ULS} : *Moment in the ultimate limit state (ULS).*

$\sigma_{m\,z}(x)$: *Equivalent stress of the ULS moment, in the z direction.*

x : *Radial distance from the center of the ring to the point of acting stress.*

I_{cube} : *Moment of inertia of the ring.*

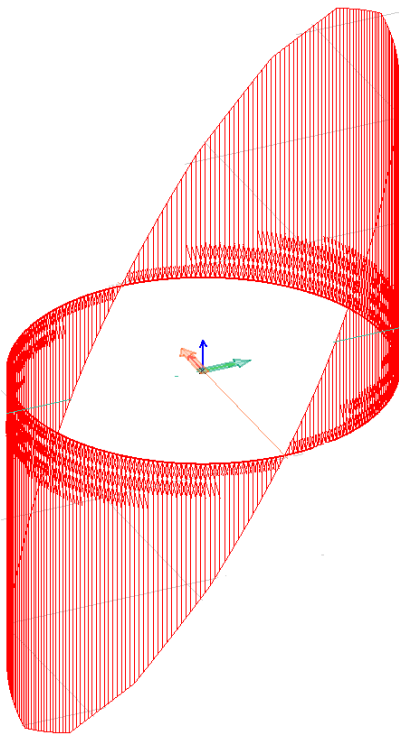r_1, r_2 : *Inner and outer radius of the ring.*

Figure 3:8 The bending moment as an applied force, varying linearly over the tower flange. The blue arrow being z direction.

3.6 Results regarding local pressures under the tower flange

The areas of highest interest for the objective are the areas with the highest stress in each material. These areas are the ones closest to the tower flange, as this is where the stress is applied.

Figure 3:9 shows a contour plot of the compressive principle stresses in the model, in this representation the extreme pressures in the steel are made black. This shows the force distribution over the cross section including the grout and plinth. The stress fairly concentrated in the grout but quickly evens out towards the horizontal grout-plinth connection. The same effect is present in the plinth to base transition.
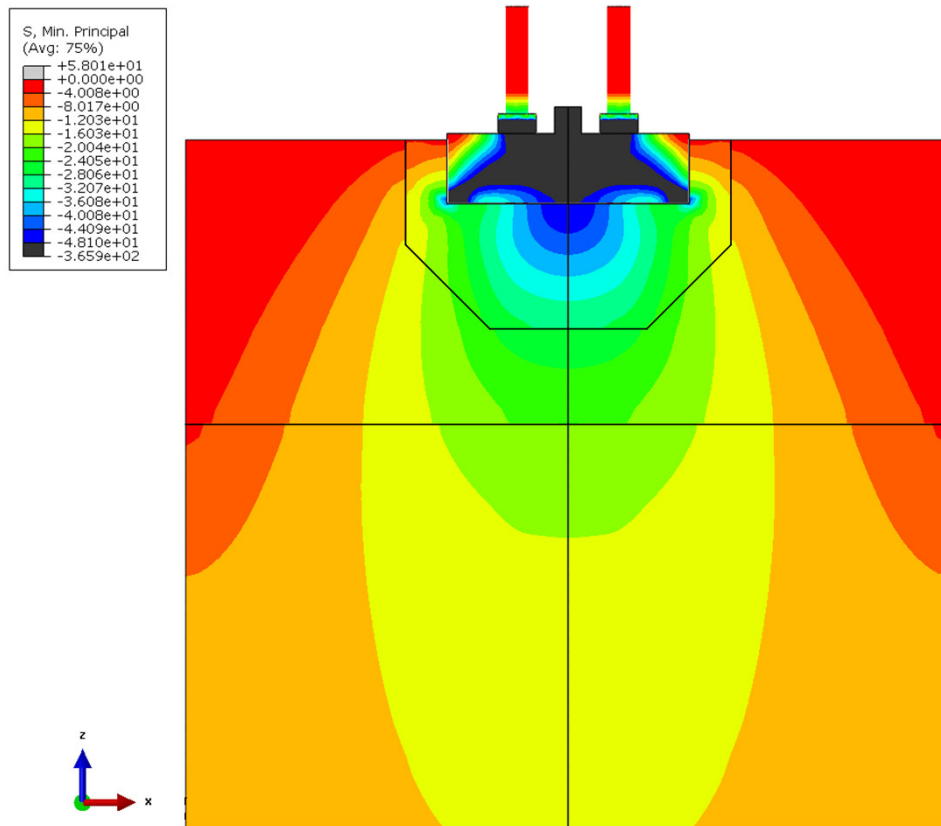
Figure 3:9 Principle compressive stresses in the top part of the model, with the black parts as extreme steel values above 48MPa.

3.6.1 Grout

Under the tower ring, the highest stress was recorded. With this in mind, the grout is also the part with the highest strength concrete, $f_{ck} = 90\ MPa$. For comparison the stresses were also plotted before the applied load was active i.e. only during the bolt load.
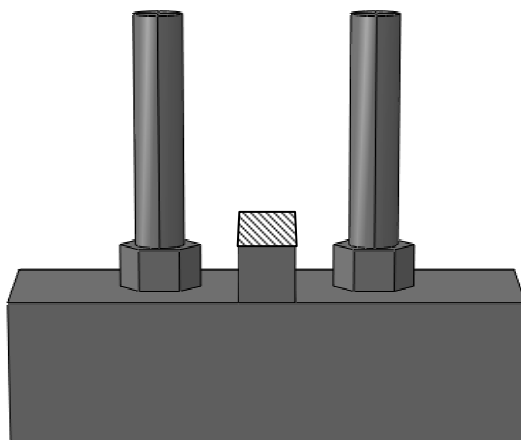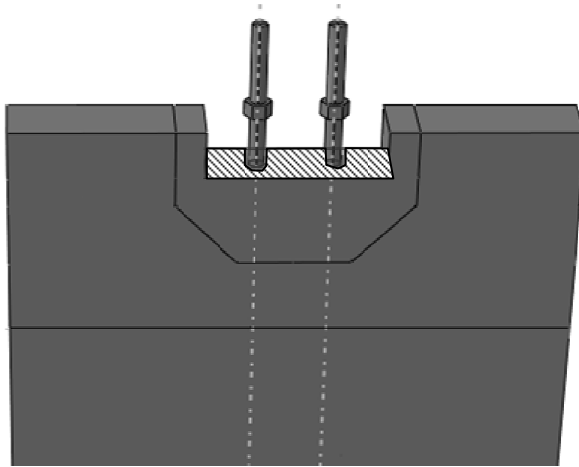

Figure 3:10 The flange, where the force is applied, highlighted with a bright hatch.

The stress is presented by three paths, a line which extracts all nodal values along its length. These paths are shown in Figure 3:12 in the area of interest as shown in Figure 3:11.

Figure 3:11 The full bolt-pair model, shown without the flange. The area of interest highlighted with a bright hatch.
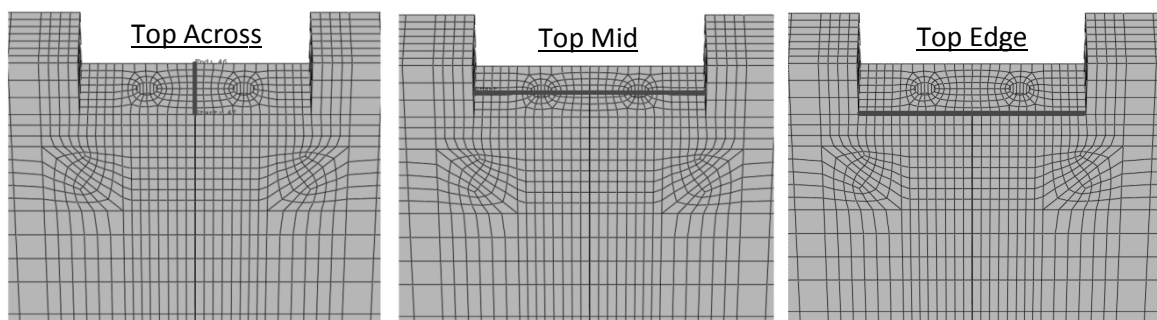
Figure 3:12 The two paths, named "Top Across" and "Top Mid" respectively.

Figure 3:13-3.16 presents the compressive principal stresses and it is clear along the path *"Top Across"* the stresses are very evenly distributed, which is also visible when looking at the various small differences along the *"Top Mid"* and *"Top Edge"* path. In Table 3:1 the maximum stress and the degrees of utilization are shown for each material.
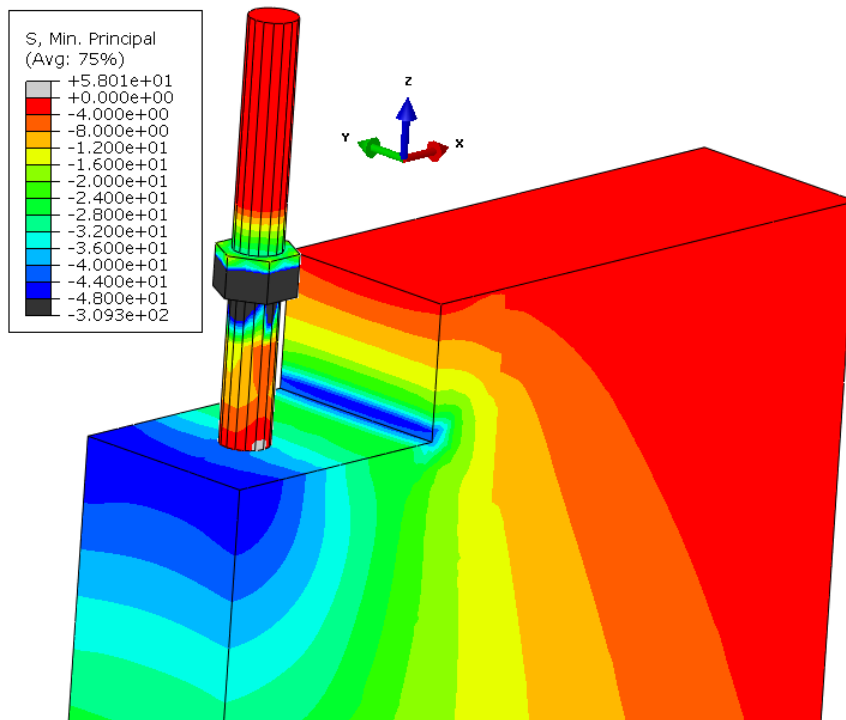
Figure 3:13 Principle compressive stresses along the models symmetry line (steel plate removed), with the black parts as extreme steel values above 48MPa.
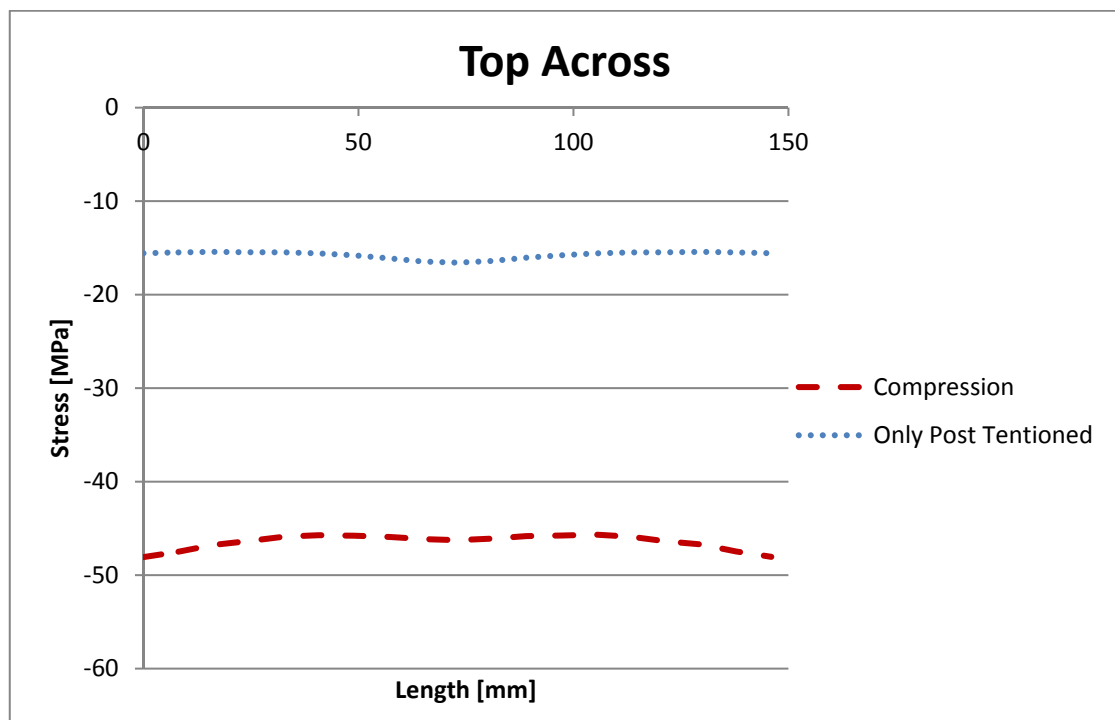

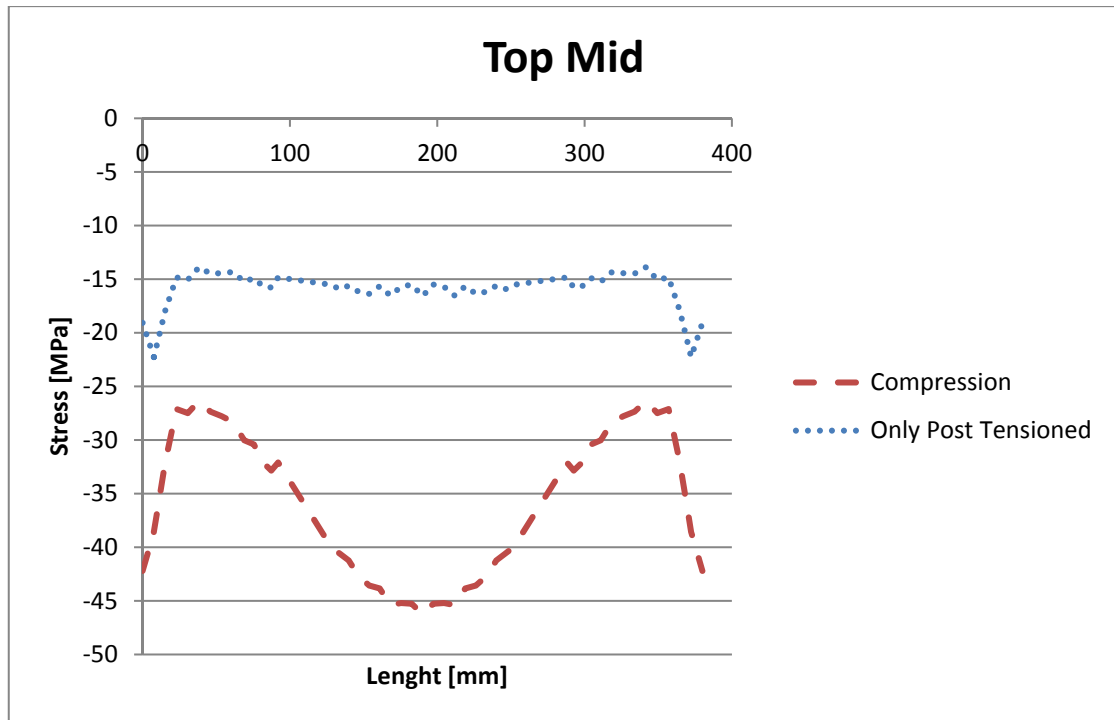*Figure 3:14 Compressive principle stresses along the path "Top Across".*

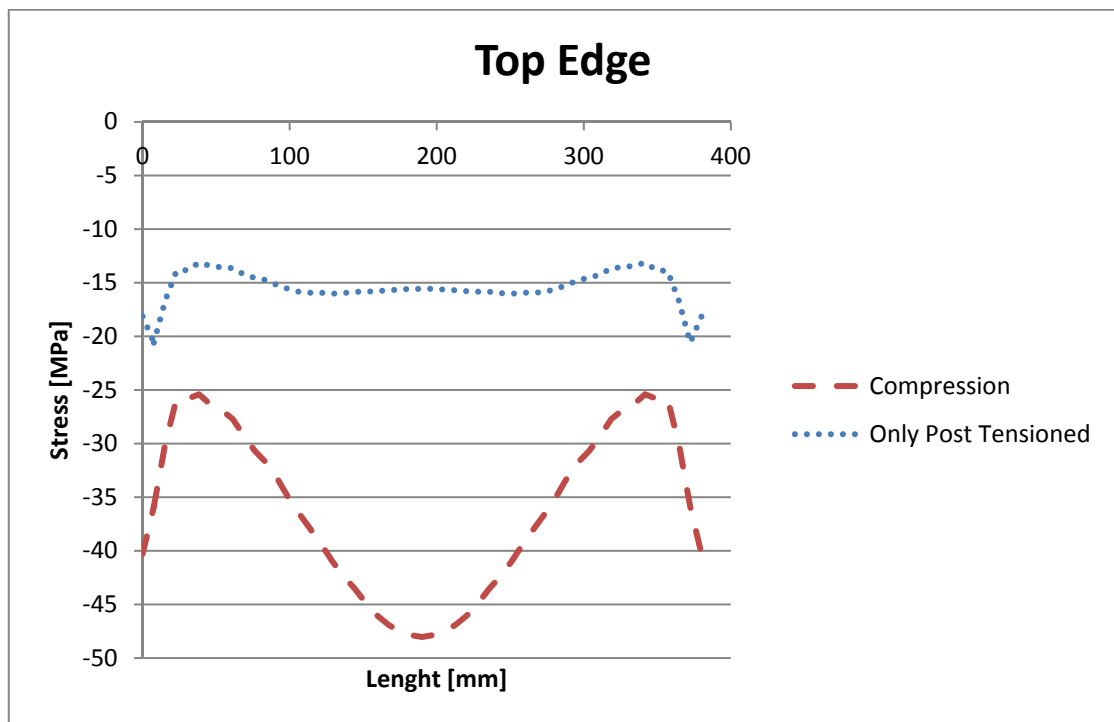*Figure 3:15 Compressive principle stresses along the path "Top Mid".*

Figure 3:16 Compressive principle stresses along the path "Top Edge".

Table 3:1 Extreme values and degree of utilization in ULS for the grout Top -paths.

	Compression	Only Post Tension
σ_{TopMid} [MPa]	-46	-22
$\sigma_{TopAcross}$ [MPa]	-48	-17
$\sigma_{TopEdge}$ [MPa]	-48	-21
$\sigma_{max} \gamma_c / f_{ck}$ [%]	80	37

To demonstrate the stresses dissipating over the depth of the grout, the stresses are extracted from the two paths *"Grout Hole"* and *"Grout Centre"* running parallel to each other and shown in Figure 3:17. The paths are drawn from the top down, and in Figure 3:18 -19, from left to right. In Table 3:2 the maximum stress and the degrees of utilization are shown for the paths.
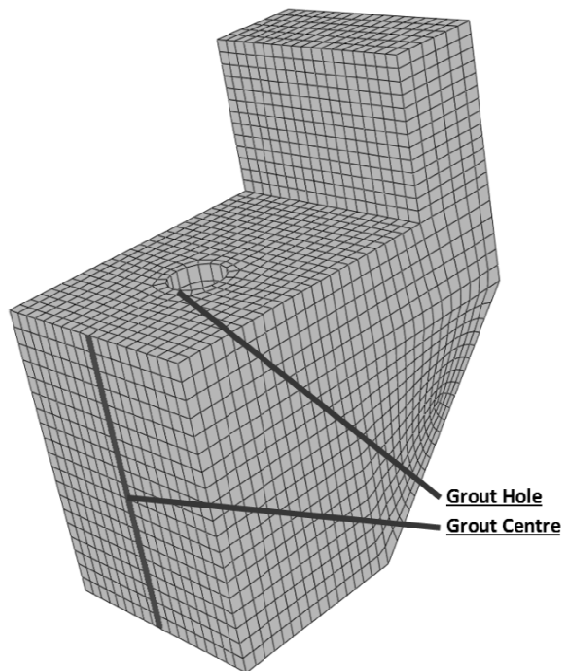

Grout Hole
Grout Centre

Figure 3:17 Path definitions in the grout. Note that the Grout Hole path passes through the hole side, parallel to the Grout Centre path.
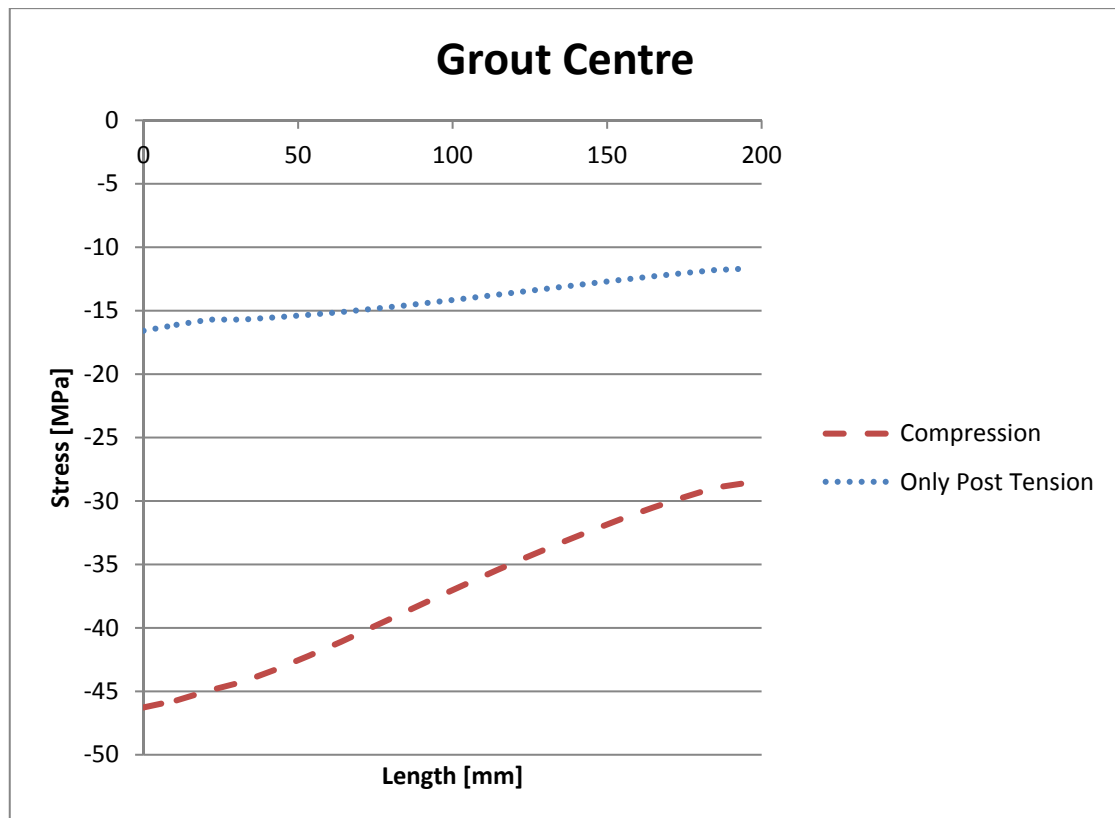
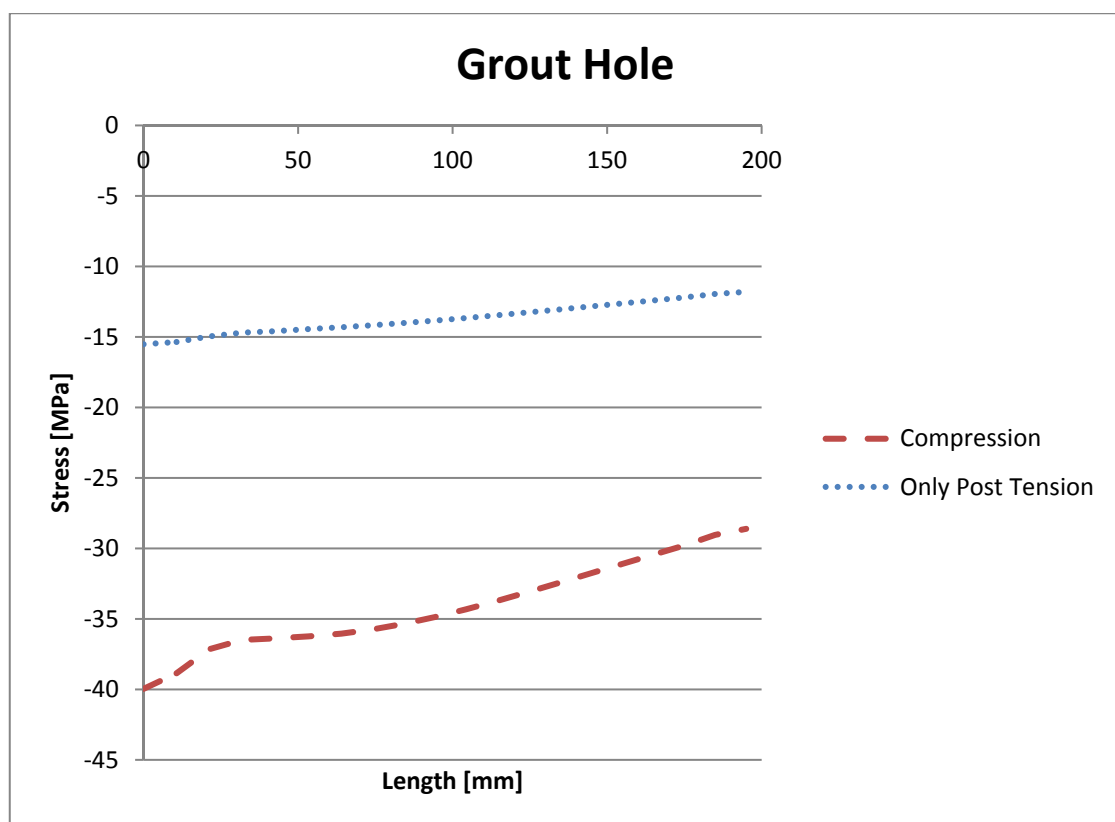*Figure 3:18 Compressive principle stresses along the path "Grout Centre".*

Figure 3:19 Compressive principle stresses along the path "Grout Hole".

Table 3:2 Extreme values from the grout -paths.

	Compression	Only Post Tension
$\sigma_{GroutCentre}\ [MPa]$	-46	-17
$\sigma_{GroutHole}\ [MPa]$	-40	-16
$\sigma_{max}\gamma_c/f_{ck}\ \ [\%]$	76.7	28.3

3.6.2 Plinth

Where the grout ends the stresses transfers in to the plinth. In the same principle as for the grout, the highest recorded stress are acting closely to the applied load from the tower, in this case in the contact zone between the grout and plinth, the plinth being of interest because of the weaker concrete class used, $f_{ck} = 45 MPa$.

The paths in Figure 3:20 show where the stresses were extracted from. The paths are presented in the grout, but the stress is the same in both parts in the connecting zone.
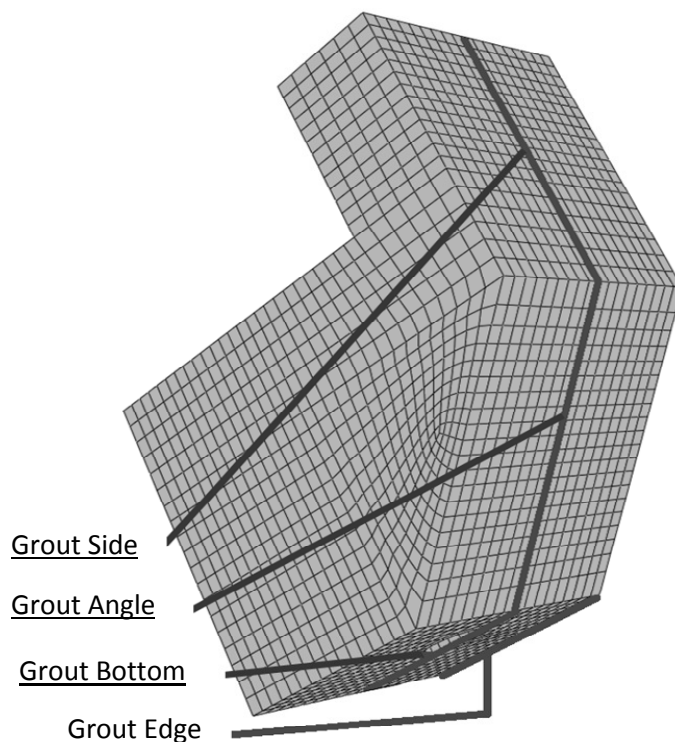

Grout Side

Grout Angle

Grout Bottom

Grout Edge

Figure 3:20 Path definitions in the grout-plinth contact zone.

Here the stress is more evenly distributed over the length of *"Grout Bottom"* than the *"Top Bottom"* indicating the stresses distributing over a larger cross section even out and dissipate. It is also evident that the stress at *"Grout Edge"* and *"Grout Bottom"* are very similar in their respective extreme values, indicating an even stress distribution.
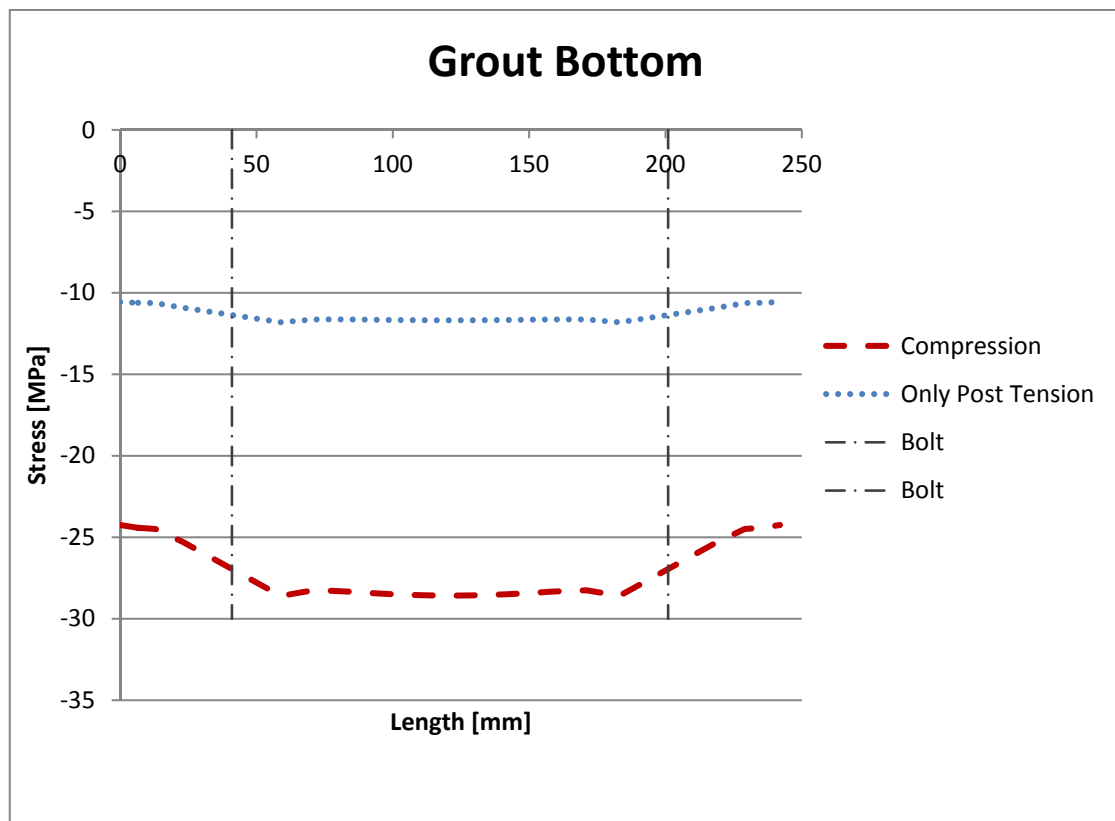
Figure 3:21 Compressive principle stresses along the "Grout Bottom" path (mirrored to illustrate the entire length).
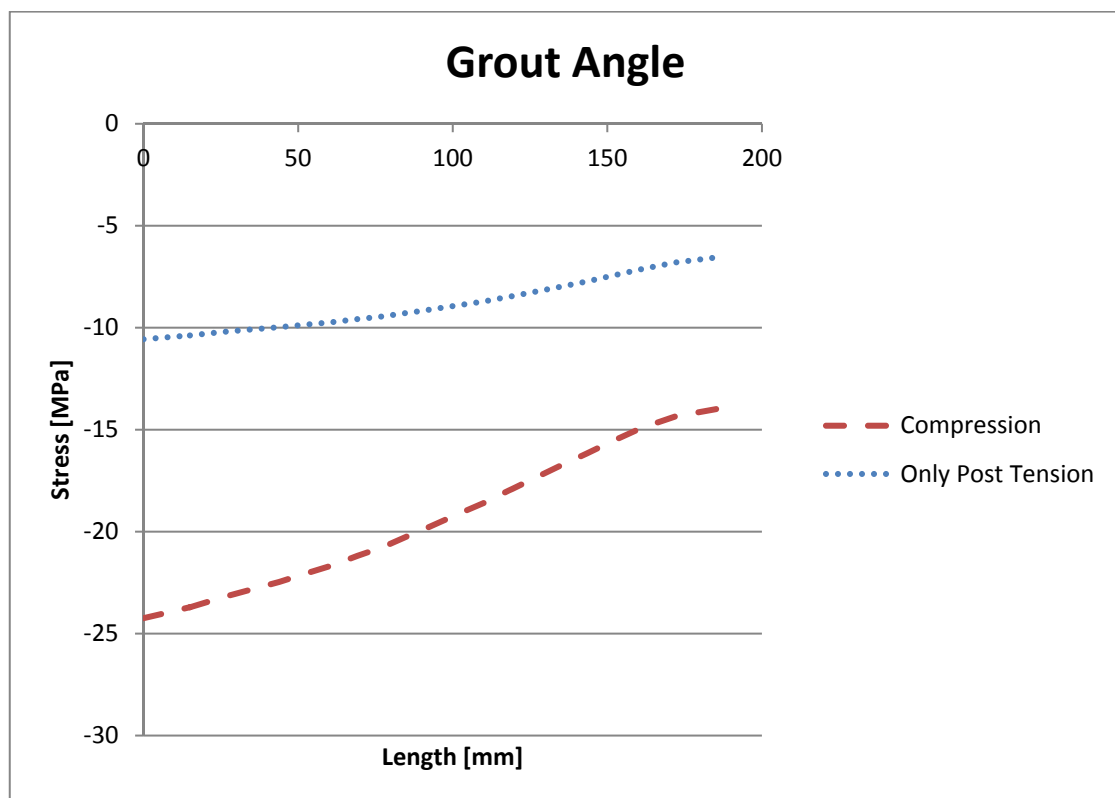

Figure 3:22 Compressive principle stresses along the path "Grout Angle".
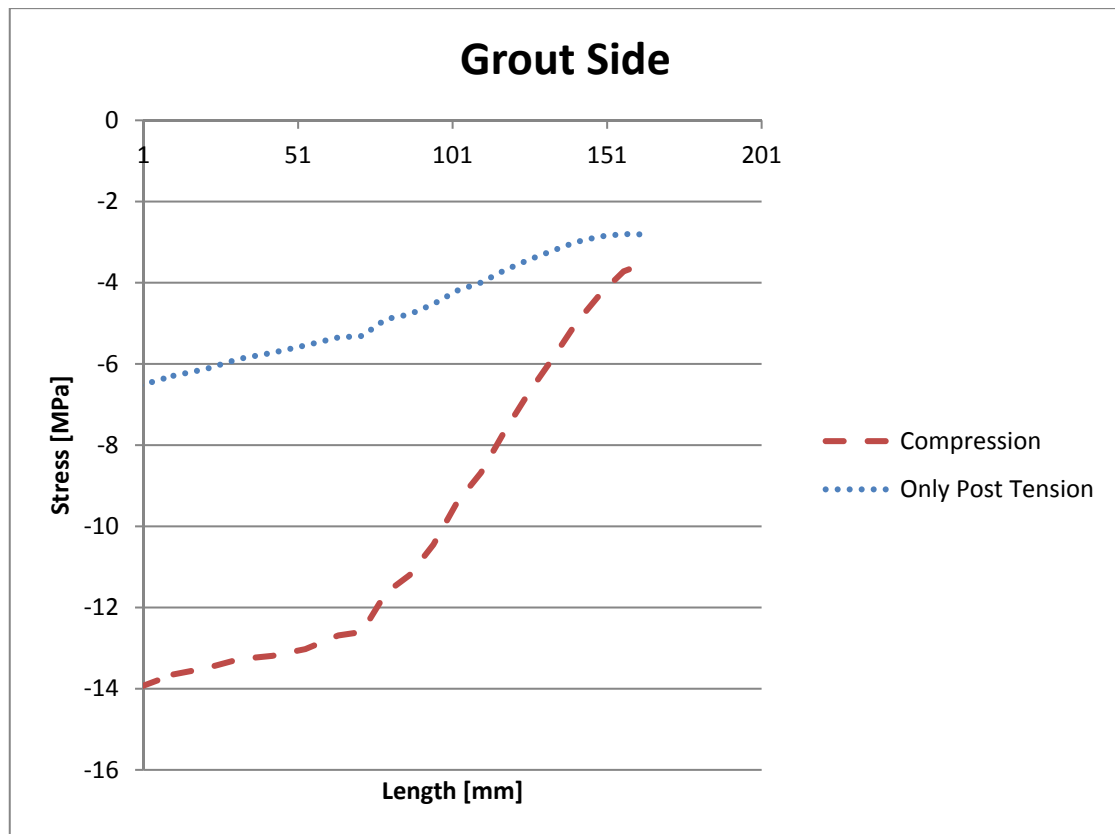
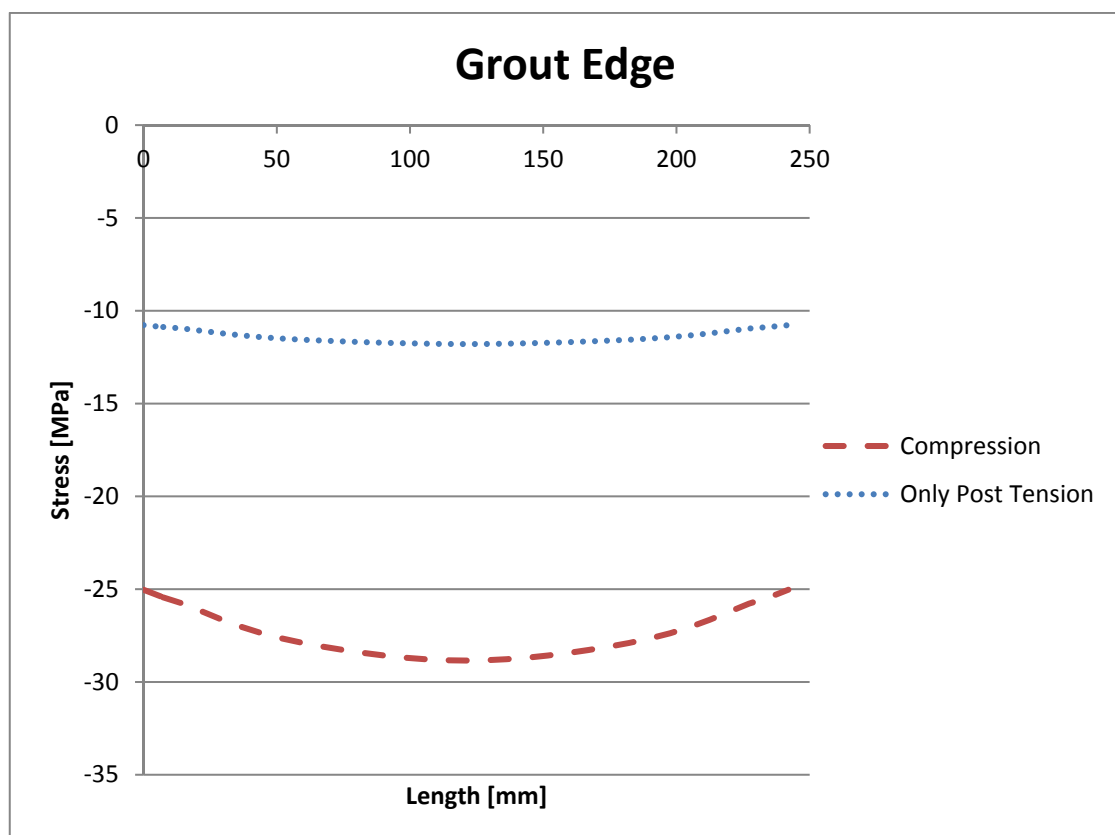*Figure 3:23 Compressive principle stresses along the path "Grout Side".*

Figure 3:24 Compressive principle stresses along the path "Grout Edge".

Table 3:3 Extreme values from the outer grout –paths in ULS.

	Compression	Only Post Tension
$\sigma_{GroutBottom}$ $[MPa]$	-27	-12
$\sigma_{GroutAngle}$ $[MPa]$	-20	-11
$\sigma_{GroutSide}$ $[MPa]$	-14	-7
$\sigma_{GroutEdge}$ $[MPa]$	-29	-12
$\sigma_{max} \gamma_c / f_{ck}$ $[\%]$	96.7	40

3.6.3 Base

In the same manner as the grout and plinth before, the highest recorded stress is acting higher up, closer to the applied load. Therefore the highest recorded stress is acting in the plinth-base contact zone, here the base is of interest since it has the weaker concrete with $f_{ck} = 32MPa$.

The paths in Figure 3:25 show where the stresses were extracted from. The paths are presented in the plinth, but the stress is the same in both parts in the connecting zone.

Plinth-Base Across
Plinth-Base Across hole
Plinth-Base Mid
Plinth-Base Edge
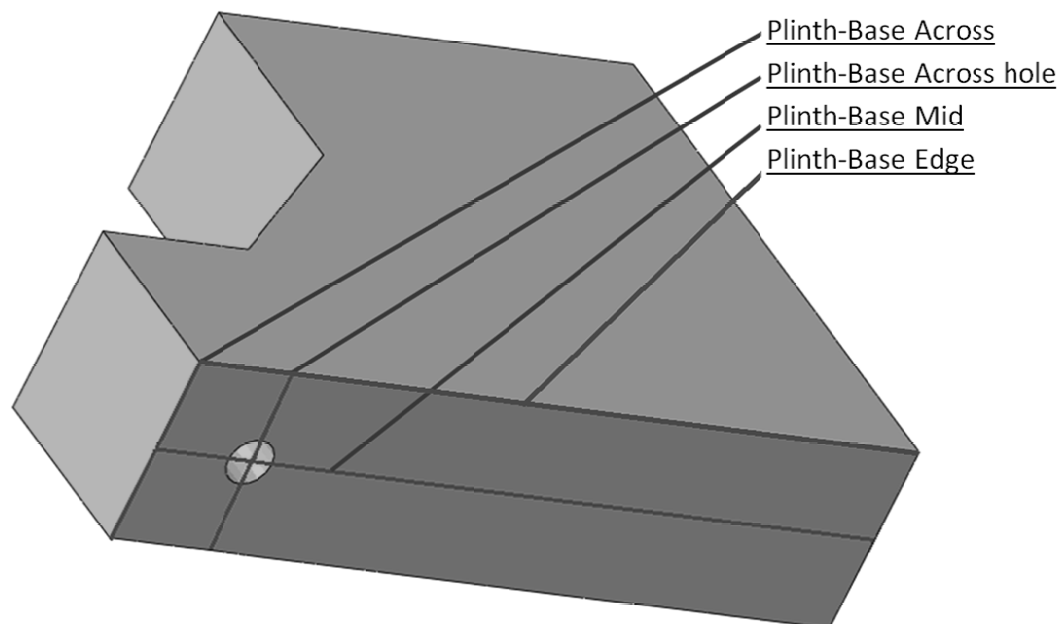
Figure 3:25 Path definitions under the plinth, in the plinth-base zone.

The results from the *"Mid Path"* and *"Edge Path"* figure were mirrored to show how the stress varied over the entire model, not just the symmetry part. This is apparent when looking at Figure 3:26 and Figure 3:29, noticing the symmetric shape over the doubled length.

Figure 3:26 Compressive principle stresses along the path "Plinth-Base Mid". The peaks come from the highly compressed areas just around the bolts.
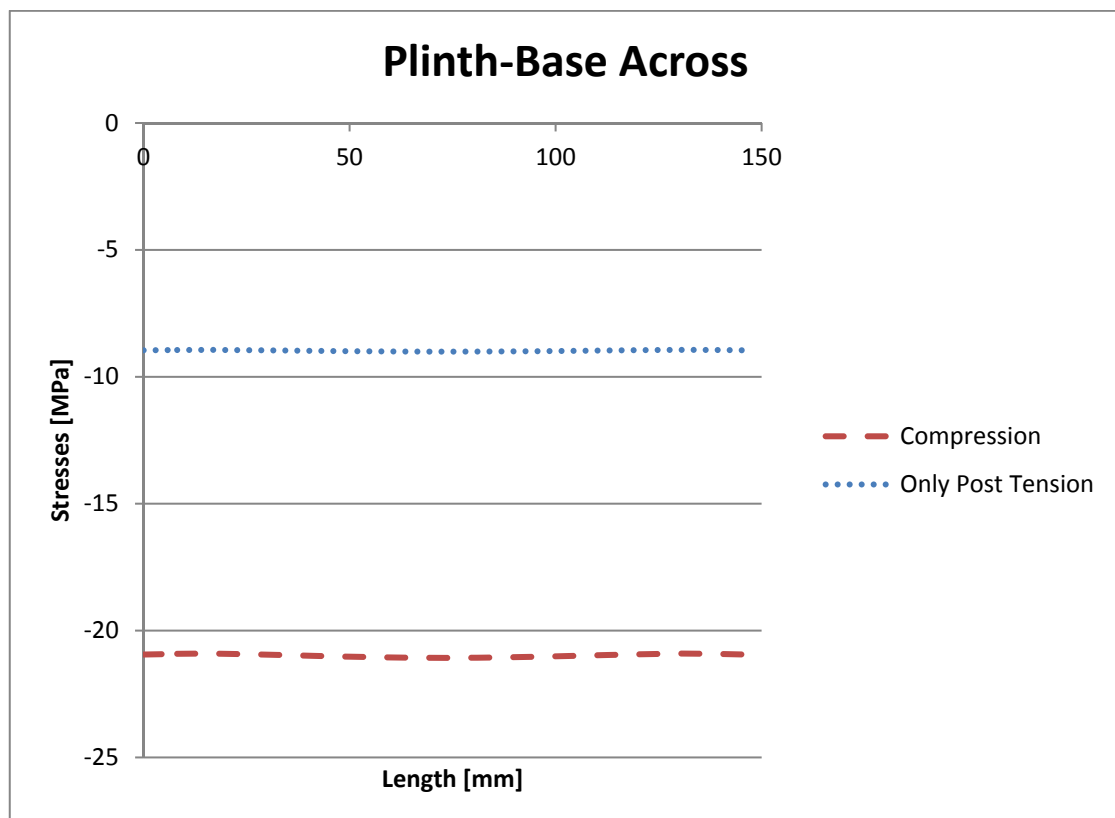
Figure 3:27 Compressive principle stresses along the path "Plinth-Base Across".

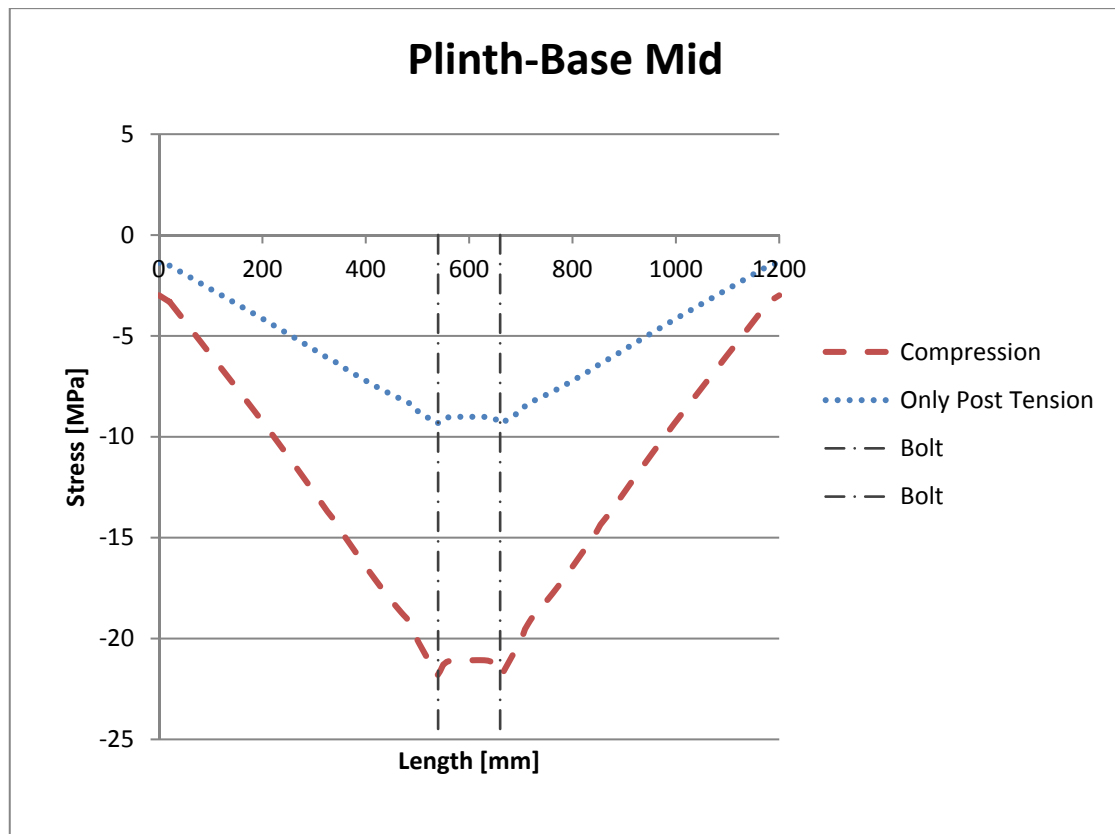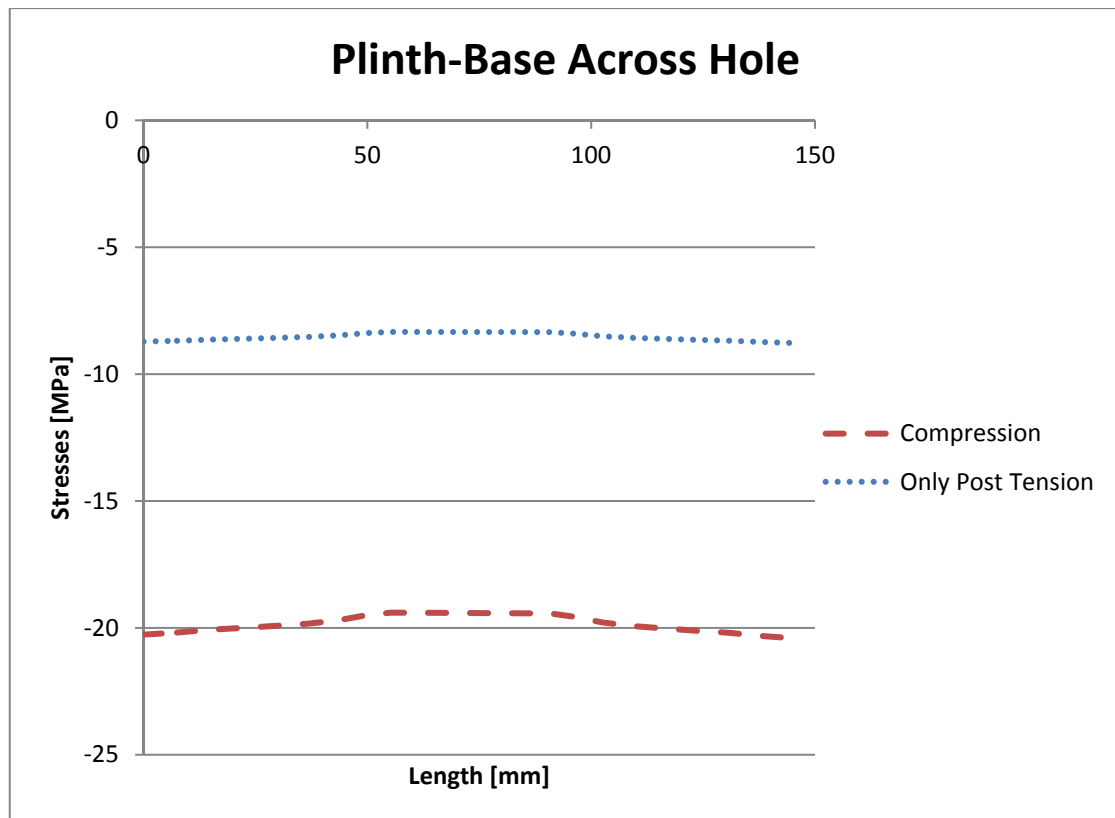*Figure 3:28 Compressive principle stresses along the path "Plinth-Base Across Hole".*
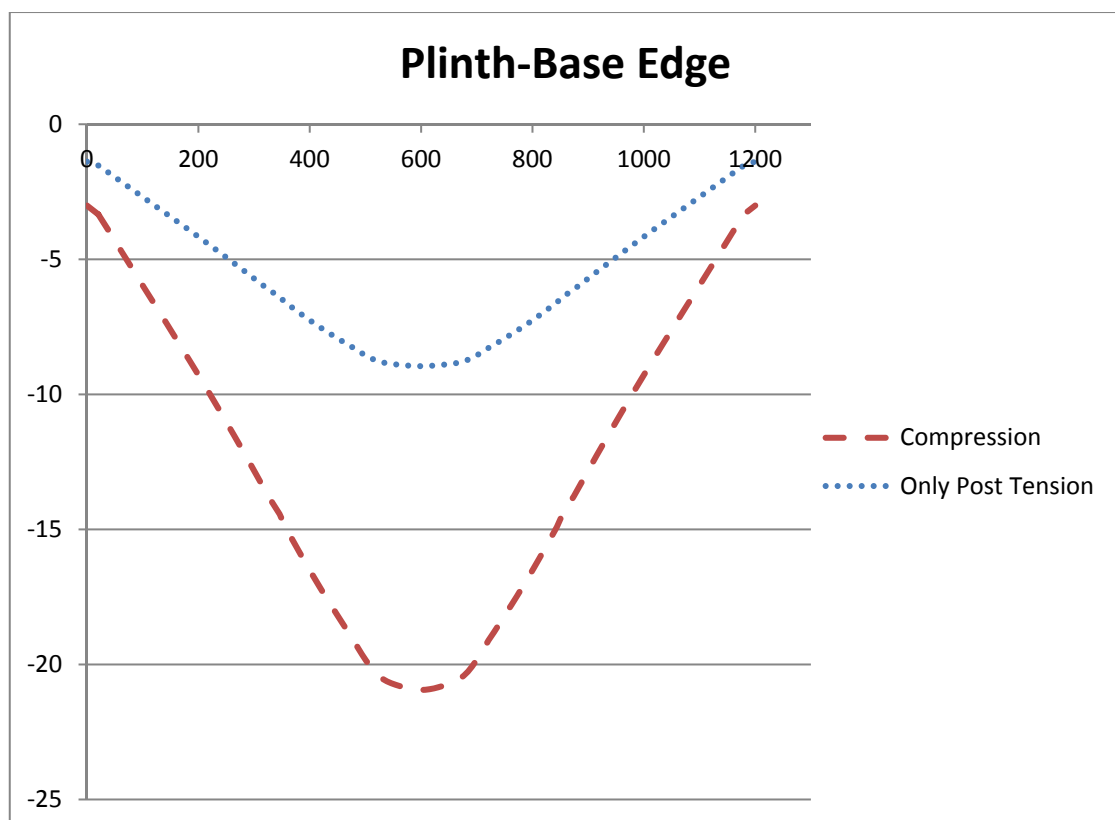
Figure 3:29 Compressive principle stresses along the path "Plinth-Base Edge".

Table 3:4 Extreme values from the plinth-paths.

	Compression	Only Post Tension
$\sigma_{PlinthBaseMid}$ $[MPa]$	-22	-9
$\sigma_{PlinthBaseAcross}$ $[MPa]$	-21	-9
$\sigma_{PlinthBaseAcrosshole}$ $[MPa]$	-20	-9
$\sigma_{PlinthBaseEdge}$ $[MPa]$	-21	-9
$\sigma_{max}\,\gamma_c/f_{ck}$ $[\%]$	103	42

4 Effect of Loss in Tension of the Bolts

This study could be performed with the same model as in Chapter 3 and therefore the results are directly presented below.

4.1 Results regarding the effect of loss in tension of the bolts

When loaded by the moment, the concrete on the compressed side of the tower is deformed. This deformation impacts the boundaries of the bolt, resulting in a tensile stress loss of the stress applied in the post-tensioning step. On the opposite side of the tower the tensile force results in a less loaded concrete, as well as affecting the post-tensioned bolts keeping the tower in place.

By extracting results from the bolt-pair model, these phenomena were studied. The results are presented in three cases: only post-tension as the active force, the compressive force in combination with the post-tensioning and the tensile force in combination with the post-tensioning.

The path for which the results were extracted runs along the centre line of the bolt and through its entire length, as illustrated in Figure 4:1.

Figure 4:1 A part of the bolt, presenting the path running along the whole bolt.
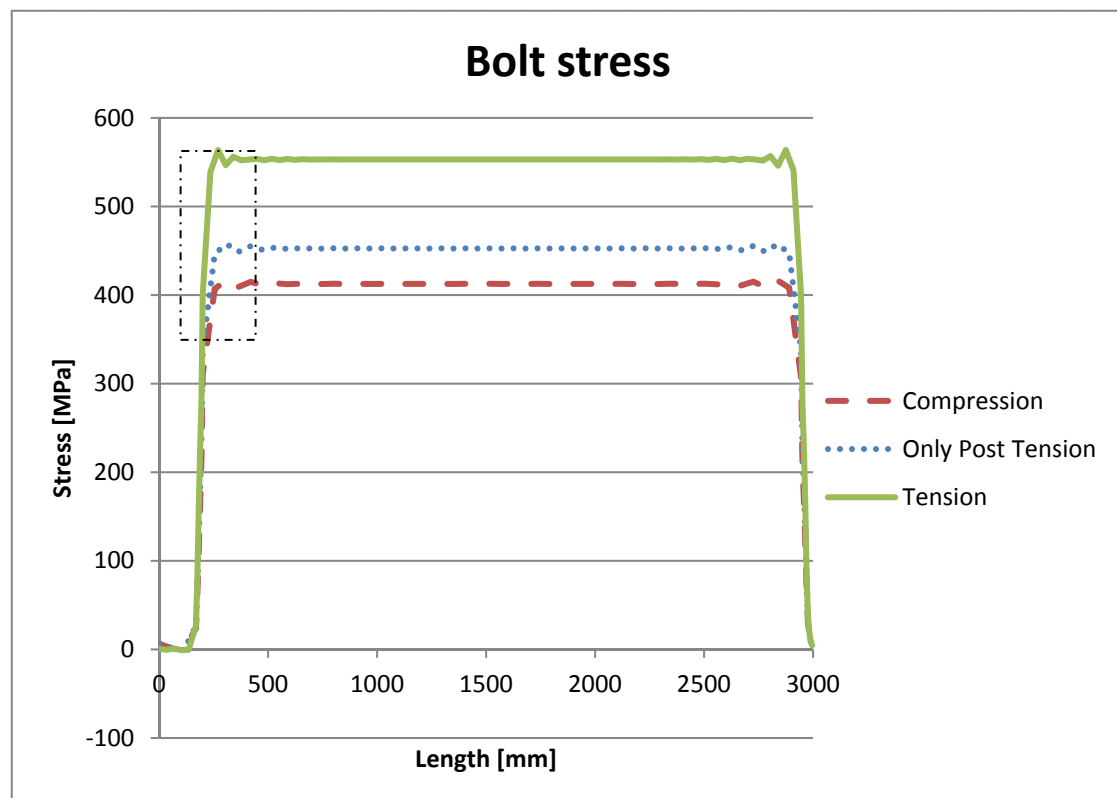

Figure 4:2 Bolt stress in the three cases, local disturbances highlighted with dash-dot.

Averaged stress in the cross section for each case, with local disturbances removed from the results, shown Table 4:1.

Table 4:1 Bolt averaged stress in the three cases.

	Compression	Only Post Tension	Tension
$\sigma_B \, [MPa]$	413	453	553
% of post tension	91.2	100	122.1

For the tensile case, the stress increases beyond the post-tensioning stress, indicating that the concrete is completely unloaded, see figure Figure 4:3. The actual state of stress in the bolts is not close to the ultimate strength of the steel, the level of which will not be disclosed in this thesis.

In the compressed case, the tensile stress reduction in the bolts due to concrete deformation is of a rather small magnitude (below 10%).
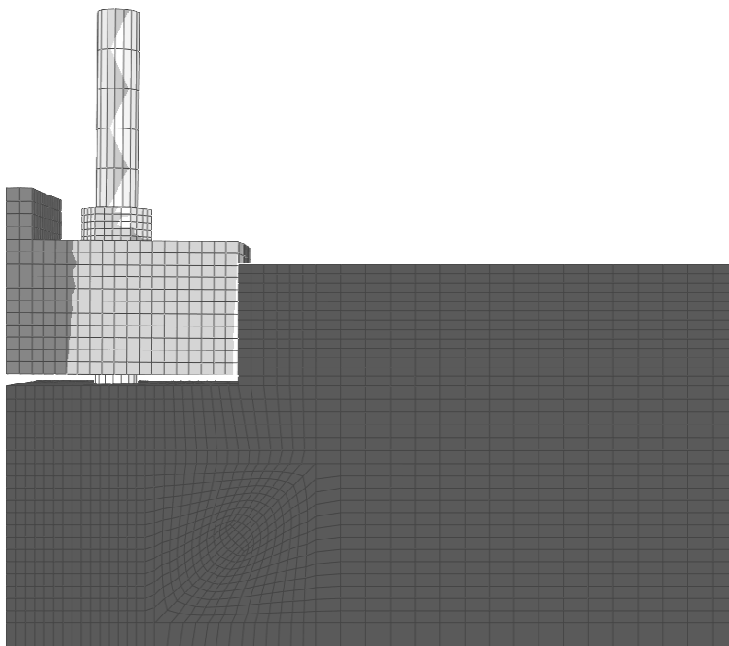
Figure 4:3 Deformations in the z-direction, for the tensile case. The top ring has "lifted" from the concrete, completely unloading it.

5 Long Term Effects

The bolt-pair model was also modified to resemble a case in ULS after 25 years of service. The influences were narrowed down to concrete creep and bolt stress relaxation. The creep accounted for by modifying the Young's modulus to an effective value and the relaxation with the post-tension stress as a base according to the (European Comittiee for Standardization, 2008).

5.1 Results regarding long term effects

The results were extracted from the same path as in Chapter 4. The results are presented in Figure 5:1 and Table 5:1.
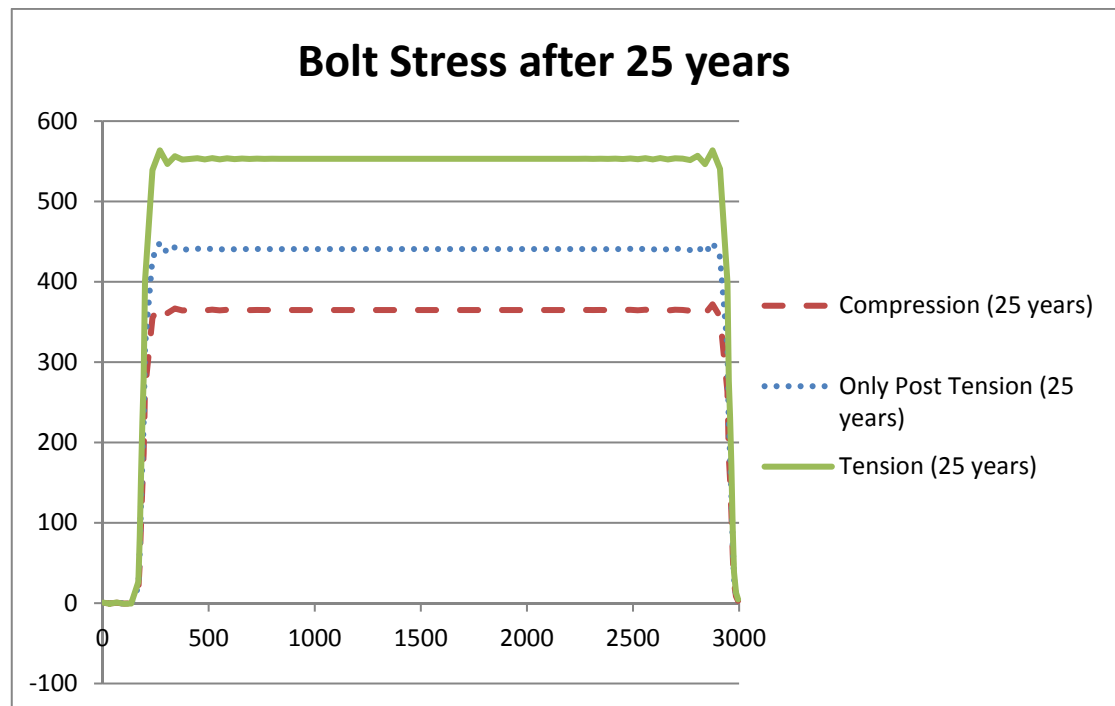
Figure 5:1 Bolt stress with the 25 year material properties.

Table 5:1 Bolt averaged stress in the two cases, after 25 years of service.

	Compression (25 years)	Only Post Tension (25 years)	Tension (25 years)
$\sigma_B \ [MPa]$	365	441	553
% of post tension	80.6	97.4	122.1
% of post tension (25 years)	82.8	100	125.4

The stress in the bolt during tension is the same as in Chapter 4, confirming the total unloading of the concrete. However, because of the stress relaxation in the bolts the ratio between the tensioned bolt stress and post-tensioned stress is slightly higher.

Since the Young's modulus decreases over time the deformation of the concrete is larger while exposed to the same stress magnitude. This affects the bolt's boundaries resulting in a lower state of stress in the bolt.

6 Identification of Areas of Interest

To identify areas of interest on both a global and local level an additional model was needed to represent global stress flow. The local stresses were presented with the bolt-pair model, described in Chapter 3. By combining the results from this new model and the bolt-pair model a more complete understanding of the anchor cage to tower connection was be formed.

6.1 Plate model

To verify the global model with the reference object, a rigid plate model in two dimensions was made in FEM-Design 13, modeling applied moment, filling and self weight of the reference object. The filling is what the soil placed upon the foundation, is called, the filling affecting this model is illustrated in Figure 6:1. The soil was represented by non-linear springs, acting only in compression. This model was verified with the reference project, where contact area and reaction forces where used as verification data.
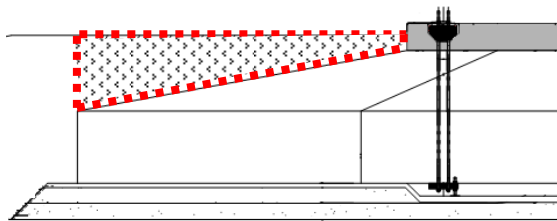
Figure 6:1 The filling over the foundation.

Figure 6:2 illustrates the internal bending moments M_x in the left figure and in the right the resulting spring forces as soil pressure, both were used to validate the model against the reference object.
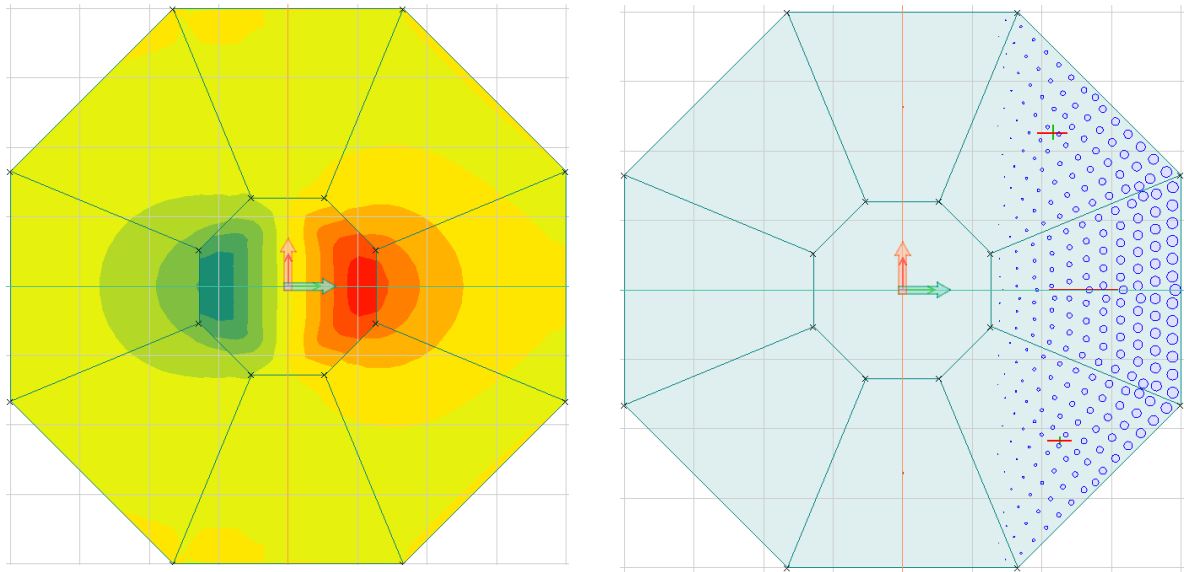
Figure 6:2 Internal bending moments, M_x, and reaction forces in the foundations, modelled in FEM-design 13.

The soil placed upon the foundation is commonly referred to as the filling and was simply modelled as a pressure varying linearly in line with the depth over the foundation edges.

6.2 Section model

The model was a full section of the shortest diameter of the foundation and had the width of the centre-to-centre distance of a bolt pair. It was modelled with a symmetry line along the centreline of the section, as shown in Figure 6:3.

Figure 6:3 The dashed section of the model, with a dotted symmetry line.

Figure 6:4 The same section in the foundation, side view.

Like the earlier models, this model represented the maximum loaded section, as shown in Figure 6:5, by using the shortest possible diameter, the model represented the maximum loaded section.

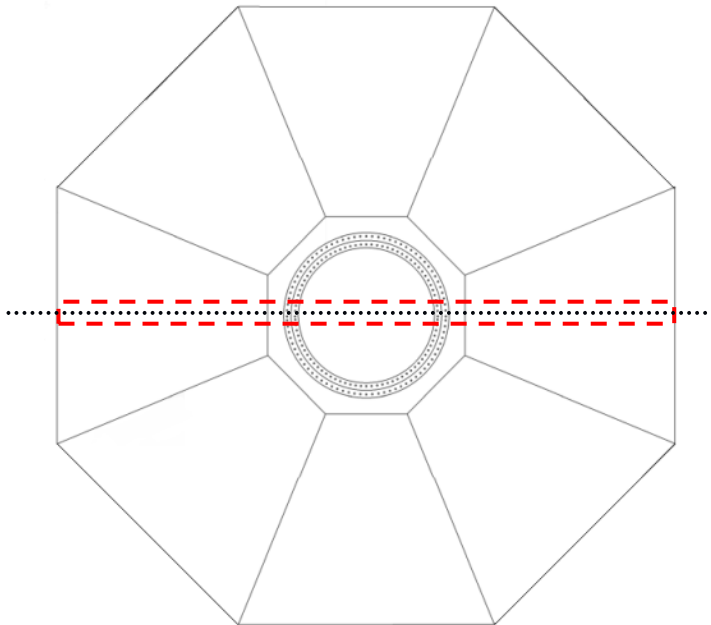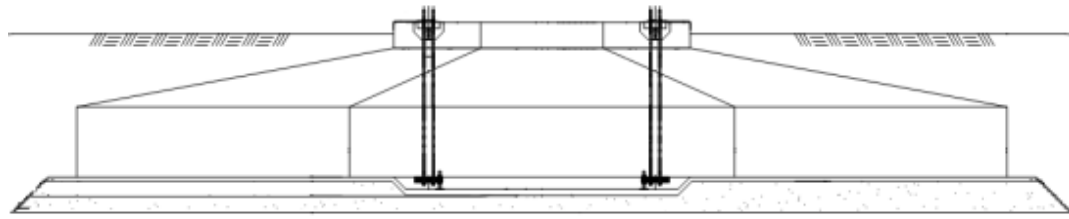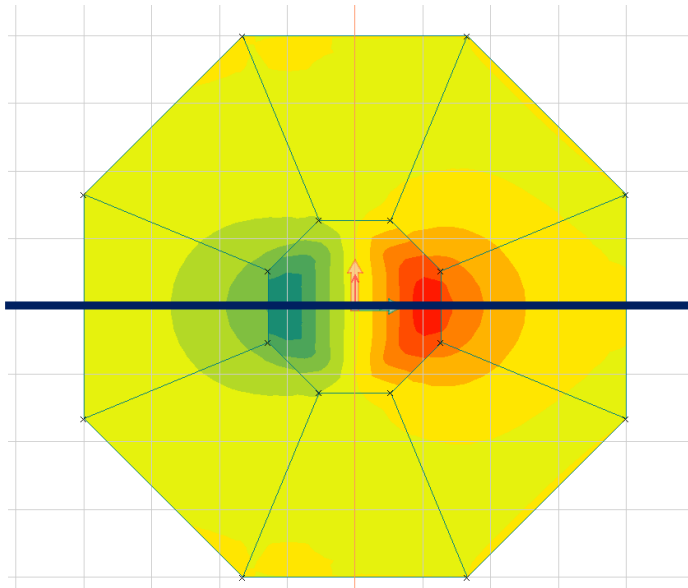*Figure 6:5 Line representing the maximum loaded section.*

6.2.1 Balancing the model

When isolating the maximum section in the foundation there were some inherent problems. The global effects of load distribution and the added resistance of a larger foundation were initially lost. This can lead to an unstable not converging solution due to extreme deformation and high loads with relation to the resisting loads.

The solutions considered were; to introduce sectional forces perpendicular to the section from an earlier analysis and therein model the resistance and effects of the foundation or to modify the input loads in the model until a balance with regard to the reference plate model is met. The latter was used in this thesis.

By modifying the external forces and the self weight to have the same total *soil pressure*, *axis of rotation* and *force resultant* as the same section in the plate model treated in Chapter 6.1, the section was considered principally correct on a global level.

6.2.1.1 Total soil pressure

Since the section model was not affected by the whole foundation, the total soil pressure was less than in the plate model. By increasing the gravity force, the model loosely represents the weight of the area close to the section, as shown in Figure 6:6.
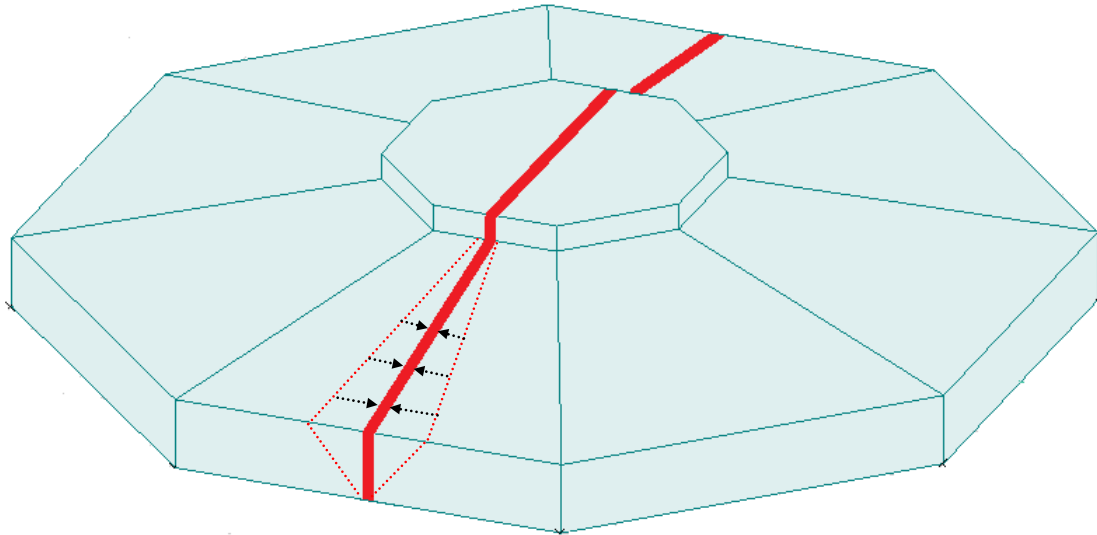
Figure 6:6 Effect of surrounding areas.

6.2.1.2 Axis of rotation

The axis of rotation is where the springs shift from passive to active, i.e. where the soil shift from non-loaded to compressed.

Like the gravity, the external forces are balanced to represent the force distribution from the maximum force section to its surrounding, less loaded sections. By decreasing the ULS moment and the WPP self weight, until the axis of rotation was the same as in the plate model, the external forces were considered roughly correct.

6.2.1.3 Force resultant

To ensure that the forces were acting on more or less the same area on both the plate and the section model; the force resultants where compared. Since the soil pressure is linear in the plate model, as illustrated in Figure 6:7 and Figure 6:8, the force resultant was easy to calculate.
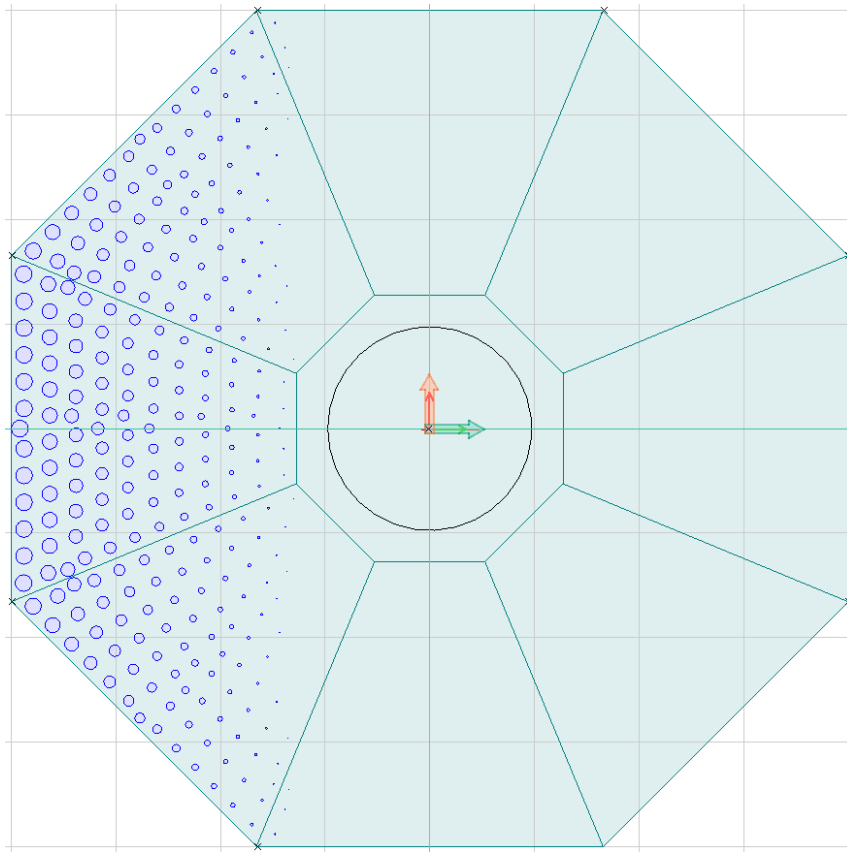
Figure 6:7 Spring forces in the foundation, as in Chapter 6.1.
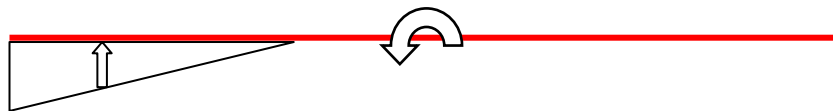
Figure 6:8 Schematic force resultant.

However, in the FE model the distribution was not as linear, because of the elastic material and geometric force concentrations. Balancing modifying the input forces to match them was a tedious task and was done by iteration. The end result is shown in Figure 6:9 with the force resultant marked as triangles while the lines represent the stress distribution over the length of the foundation.

Figure 6:9 Force distribution under the compressed part of the slab.

6.2.2 Soil

Soil data from the reference project was applied to the model in four different manners; *springs* at nodes, as a *solid material,* as an e*lastic foundation interaction* and with the *spring-to-grou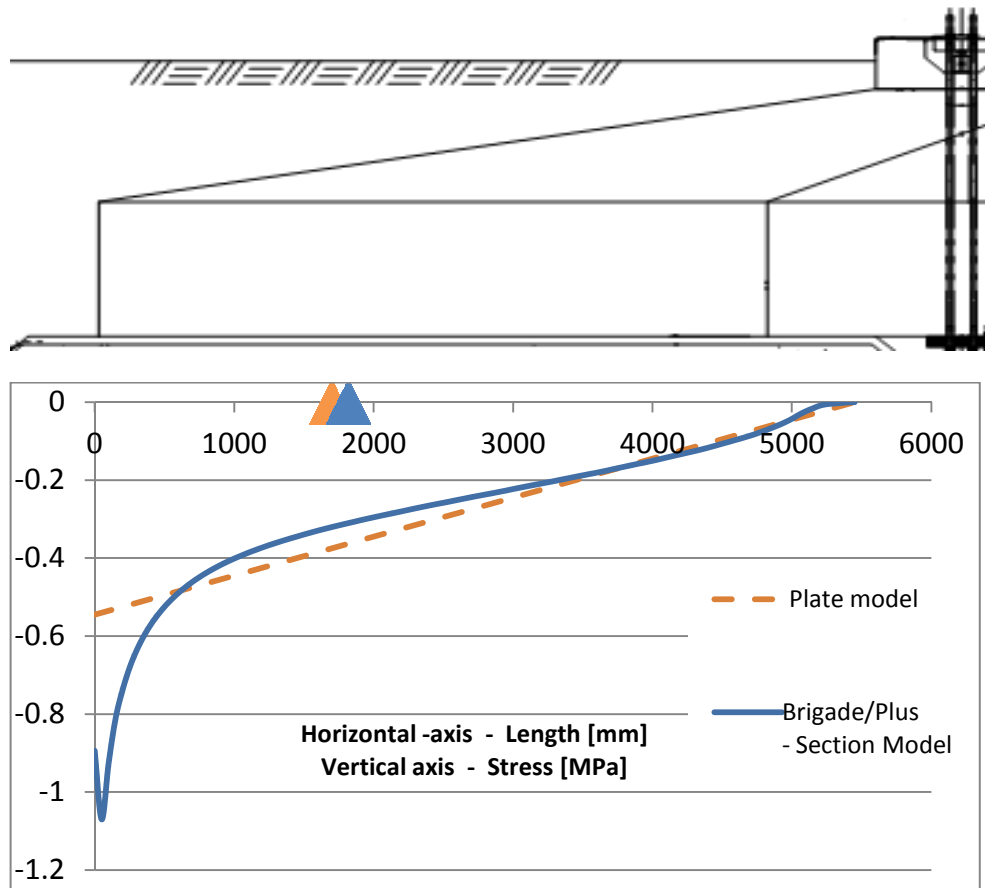nd* module in Brigade/Plus. All of them had their pros and cons, mainly modeling wise, but also in representation of reality. They were all based on the E-modulus of the soil, a crude simplification of the soil, but suitable for the model.

- *Springs* – By assigning a spring to a set number of nodes, e.g. a line of nodes, the springs can be controlled to represent the soil. The spring stiffness was calculated as: $k_{spring} = E_{soil} * A_{element}$. The foundation was considered stiff enough to only need a line of nodes, from the edge of the foundation to the pivot point of the foundation. This was due to the fact that the springs were not non-linear, i.e. could not be set to only act in compression. This lack of non-linearity lead to some problems, mainly an additional parameter to iterate. The process of collecting data was also quite cumbersome. All information of interest from the springs had to be assigned in the step module, before computing the model. Compiling the output data from the springs into curves was time consuming since the data was given spring-wise instead of a list with all nodes, therefore the method was not used.

- *Elastic foundation interaction* – This interaction condition is native to ABAQUS and is assigned to a surface, which in turn is assigned stiffness per area, i.e. the Young´s modulus. This is supposed to work as a spring bed with the spring acting against the normal of the applied surface (Dassault Systèmes, 2012). Due to difficulties to verify the reaction forces, this method was not used.
- *Spring-to-ground* – A Brigade/Plus module developed by Scanscot. Works as a combination of the spring method and the elastic foundation interaction method. Just like the elastic foundation interaction method a surface is assigned stiffness, but then the surface is automatically assigned springs to each mesh node. The difference is that instead of a surface with springs acting against the normal of the surface, one global direction has to be chosen (x,y,z), as well as rotational degrees of freedom, which are not affected by the elastic foundation interaction. This module had a tendency to crash frequently and was therefore very difficult to use and not reliable.
- *Solid material* – A solid with the same Young´s modulus as the real soil was modeled underneath the foundation, acting as soil. This was harder to calibrate, but in turn easier to compile data, since this could be done just by using the nodal data from the solid itself. By using the correct contact condition it was also possible for the soil to only act in compression.

Even though all methods where useable, the choice fell on the solid material method of modeling the soil. This was mainly because of the simplicity of collecting output data and its ability to only act in compression.

6.3 Results regarding identification of areas of interest

In this chapter, only the global stress flow is presented, since the local stress flow was presented in Chapter 3. As earlier described, the magnitudes were not realistic; however the force pattern was representative of the true foundation behavior.

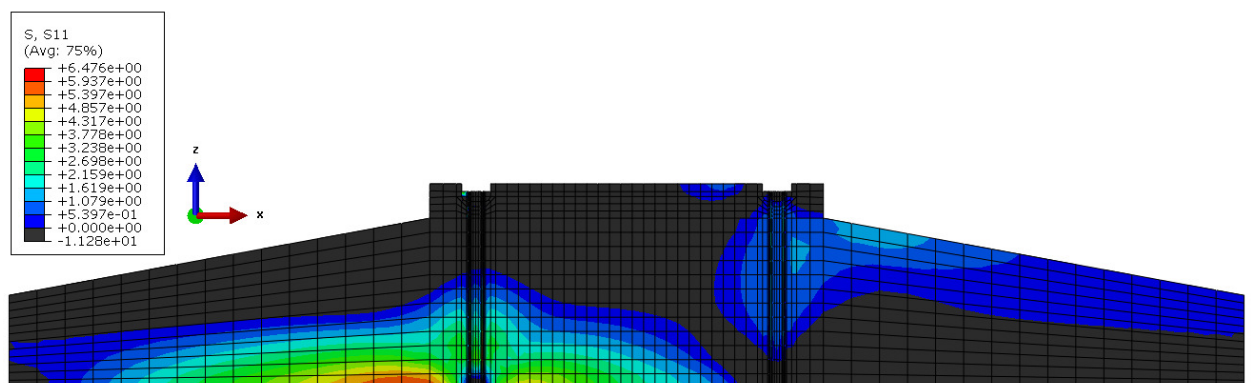*Figure 6:10 Stresses in MPa along the X-direction, only tensile values plotted in colour.*
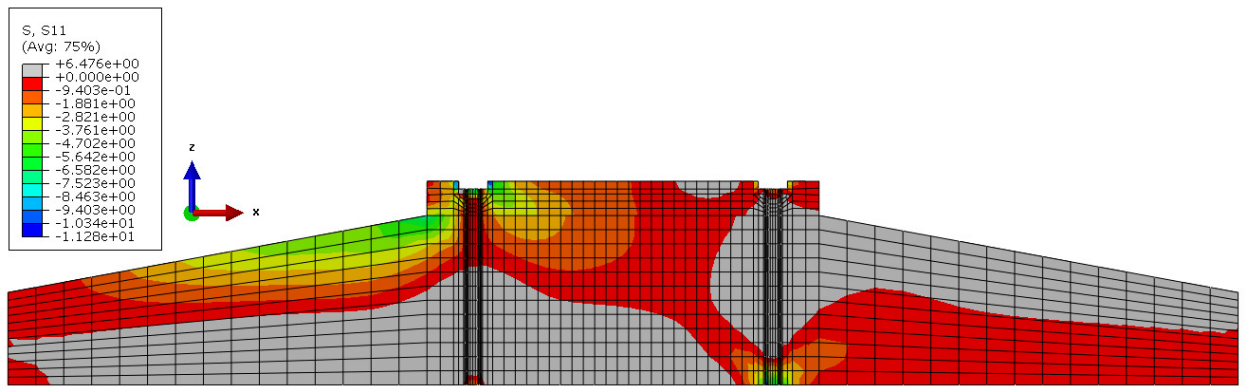
Figure 6:11 Stresses in MPa along the X-direction, only compressive values plotted in colour.
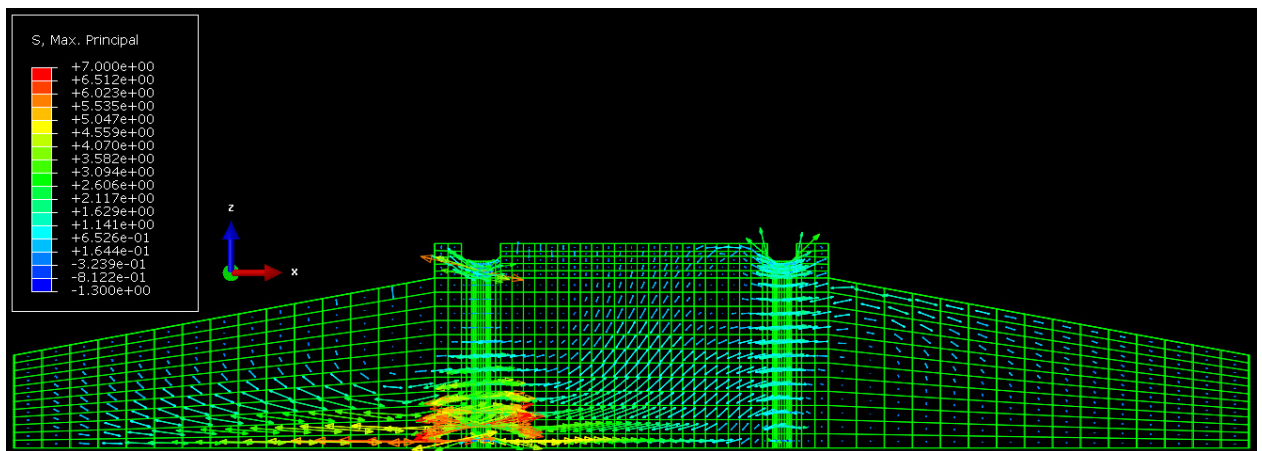

Figure 6:12 Schematic picture of the stress flow through the foundation in tensile principal stress.
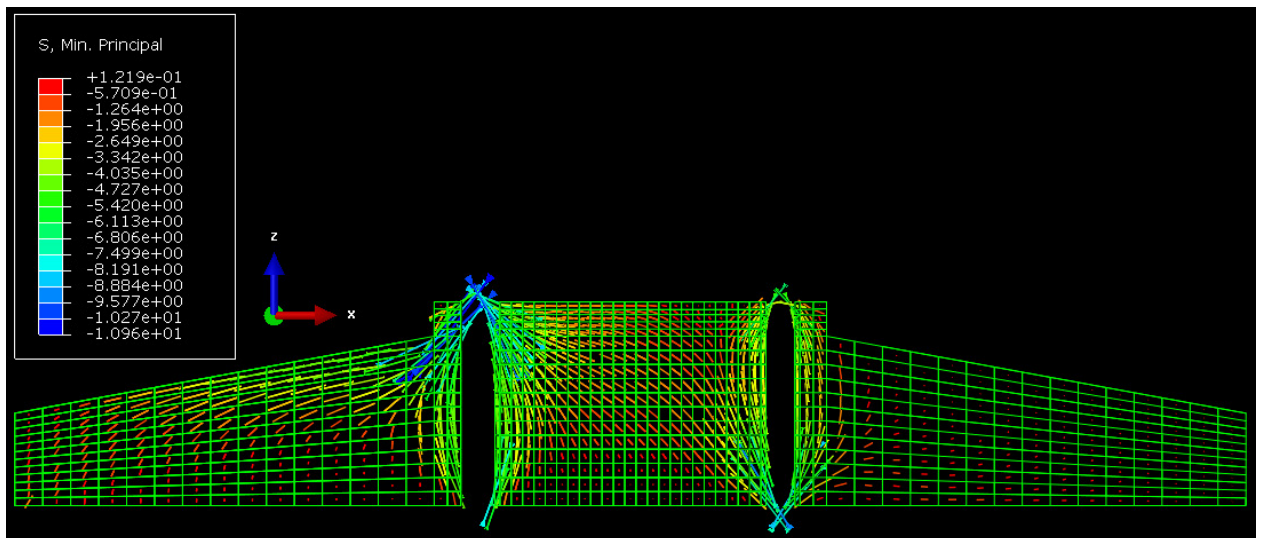

Figure 6:13 Schematic picture of the stress flow through the foundation in compressive principal stress.

7　Discussion

A general discussion follows with focus on the aims and objectives but also on general thoughts regarding the study.

> *Analyze local pressures in the concrete under the tower flange, with focus on material strength in the grout, plinth and plinth-base contact zone.*

When examining the maximal stresses through the model, it is evident that the pressure does not come close to the design value of the concrete in all but one case; in the plinth base connection. Here the values are just above the allowed design, however there are two major points to this. Firstly this is a bit "down" in the foundation and as discussed earlier, the bolt-pair model has its strength in local analysis and this area should be positively influenced by its neighbouring materials. With this in mind the pressures in this section might be lower. Secondly and more importantly, the plinth and the base are cast together at the same time, the zone in between is not a clear line and the pressures just exceeds the design value with 3%, in reality this might occur in a part where it actually is higher strength concrete in place. And lastly, confined concrete is more resistant to compressive forces and is allowed a higher load in design.

It is also interesting looking at the maximum degrees of utilization. The grout has substantially lower degree of utilization than the plinth and base. This might have to do with the fact that Vestas supplies the grouting concrete, were the total cost of the grouting is low, relatively the tower, wings and nacelle.

The bolts are generally loaded with stresses far below their designed yield limit, and are kept well within the elastic zone.

> *Study the effect of loss in tension of the post-tensioned anchor bolts during extreme loading.*

In the compressive analysis, the bolt load is still active in the most extreme case of loading, i.e. even though that the tower compresses the concrete, the bolt tensioning still secures the tower down to the base. An elastic loss of about 9%, see Table 4:1 which is not significant. However, on the tensile side of the tower, the concrete is completely "unloaded" from the post tensioning force and the bolt is only loaded with the tensile force from the tower. This might lead to some fatigue related problems not discussed in this thesis.

> *Study the long term effects on the post-tensioning force.*

The material is less stiff after 25 years and thus there are larger material deformations with the same stress and larger deformations leads to less post-tensioning force on the compressed side of the moment. The material relaxation in the bolt together with the concrete creep reduces the post-tensioning force in all bolts, on all sides of the foundation with about 2.5%.

Combining local and global analyses to identify areas of interest for structural design.

The main global stresses influencing the upper ring connection, are the foundation bending induced compression and tension stress. At the compressed bolt pair this the bending induces additional compression, increasing the total stress. However, since it acts in a biaxial manner the concrete might have a higher stress resistance in this area. At the tensioned bolt pair a small tensile area can be observed, this should be handled by the reinforcement in the area.

Also a compressive strut forms between the bottom of the tensioned side and the upper compressed side, as seen in Figure 6:11 and Figure 6:13. This strut compresses the compressed bolt pair from another direction, resulting in an even higher state of stress.

Evaluate the suitability to use advanced finite element modelling (FEM) as an analysis and design tool of wind power plant foundations.

3D finite element analyses proved a very powerful tool to analyse local problems, especially when combining a sequence of events such as different load combinations. As the time to create and compute models, increase exponentially for larger and more complex models, evaluating a complete complex structure like a WPP foundation would be very time consuming. Also, to create such a model requires a decent amount of experience of both FE-analysis and the software used.

General modelling problems

The *bolt-pair* model has some flaws that should be addressed; as it is only a small piece of the foundation, the effects of the surrounding materials are not represented, resulting in no effects of the less loaded areas neighbouring the model. It is plausible to believe that further down in the model, the stresses would spread to the surrounding areas not represented in the model. Likewise, the flange in the model is a small piece of the large ring, the ring contributes to the load carrying unit and is stiffer than the modelled region. This stiffness should lead to less deformation of the flange as well as lower compressive stresses in the flange edges.

As the boundary conditions locks a large part of the bottom part of the model, the model act as a column rather than a part of a large model, lacking global effects and internal shear. However, the local effects are considered reliable.

The *section model* has the same problems with the lack of influence from surrounding material. However the force pattern through can, after a lot of balancing, be regarded as correct and the flow usable to draw conclusions. The force pattern closely resembles a truss system with tensile ties and compressive struts.

Neither reinforcement nor non-linear material behaviour of concrete was included in the models. The combination of non-linear material and reinforcement could change the distribution of stresses compared to this linear-elastic model.

8   Conclusions

In this chapter conclusion based on the results and the discussion is presented. The general conclusion is that the anchorage cage-tower connection performs well. However, with regard to the aims and objectives, the following specific conclusions were drawn.

Analyze local pressures in the concrete under the tower flange, with focus on material strength in the grout, plinth and plinth-base contact zone.

Two main areas of interest were noted: first of, the grout has a very low degree of utilization; this was believed to be a critical area, but the results indicate that from a ULS persective, it is not. Secondly, the extreme compression stress magnitude reached in the model's plinth-base contact zone exceeds the design strength of the concrete. As discussed earlier, the strength of the contact zone can be higher than modeled, due to concrete mixing and confinement. Also, the stress could have dissipated to neighboring areas not represented in the model. Still, the area has a high degree of utilization and is thus of interest.

Study the effect of loss in tension of the post-tensioned anchor bolts during extreme loading.

Even under extreme compression the bolt pair on the compressed side of the tower is active. The tensile side, on the other hand, the concrete is not loaded, since the uplifting force from the tower is greater than the post-tensioning force. This can be problematic, but as discussed earlier, the model does not represent the less affected neighboring bolt pairs, which should have a positive effect on this bolt pair.

Study the long term effects on the post-tensioning force.

With the effective Young's modulus of concrete including creep for 25 years and stress relaxation in the bolts the results differ. The loss in tension on the compressed side is not large enough to completely unload the bolt and thus the bolt is still active, and should therefore not be critical for design. On the tensioned side however, the post-tensioning force will be even less than before, therefore creep and relaxation effects should be included in design.

Combining local and global analyses to identify areas of interest for structural design.

Global effects come into play when designing on a local level. In areas of the concrete where multiaxial states of stress exist, the tensile forces act as a negatively influencing force. These areas, specifically regarding the upper flange exposed to tension, need

careful reinforcing. The multiaxially compressed zones influencing local design is not as crucial, but still has to be taken into consideration.

> *Evaluate the suitability to use advanced finite element modelling (FEM) as an analysis and design tool of wind power plant foundations.*

To get a reliable global analysis the model has to be fairly big and, there by complex, to represent a slabs true behaviour. Because of the level of complexity; FE analysis is not a good tool for global design in these kinds of foundations. Anyhow, locally it works very well and is possible to use in design and analysis. However, as normal design has little need of specific local analysis; advanced finite element analysis is of little use for designing, while simpler easy made analysis is a good aid.

In finite element modelling, it is difficult to use a thin slice of a full model as a design and analysis tool, since this does not include three dimensional effects of the complete system. For the full representation a full three dimensional model is necessary.

8.1   Future research

A couple of suggestions of further investigations, in line with current studies are presented in this chapter.

A closer study of the bottom ring is of great interest, since the bottom part of the foundation consists of weaker concrete this could be a critical area.

To further investigate the complete force flow through the foundation a model that both resemble the magnitudes and the force pattern should be created. This model preferably is a symmetry model of the entire foundation, in varying detail; from only the concrete to one with all the bolts and the cage. From this, conclusions based on actual stress states throughout the model can be drawn.

Introducing a model which mathematically represents the influence of reinforcement, together with concrete cracking models and non-linear materials.

In situ measuring of a real foundation in use, to confirm current design, numerical models and computer models.

The influence of using a non-linear soil model, instead of linearly elastic soil model on the global force pattern and soil pressure.

9 References

Burton, T., 2011. *Wind energy handbook.* 2nd Edition ed. Chichester, West Sussex: Wiley.

Dassault Systèmes, 2012. *Abaqus Analysis user´s Manual.* Providence, RI, USA: Dassault Systèmes Simulia Corp..

Domone, P. & Illston, J., 2010. *Construction Materials.* 4 ed. London: Spoon Press.

Dowling, N. E., 2013. *Mechanical Behaviour of Materials.* 4th edition ed. Harlow: Pearson Education Limited.

Engström, B., 2011. *Design and analysis of deep beams, plates and other discontinuity regions,* Göteborg: Chalmers University of Technology.

Engström, B., 2011. *Restrain cracking of reinforced concrete structures.* Göteborg: Chalmers University of Technology.

European Comittiee for Standardization, 2008. *Eurocode 2: Design of concrrete stuctures - Part 1-1 General rules for buildings.* 1 ed. Stockholm: Swedish Standards Institute.

European Commission, 2013. *European Commission, Research and Innovation.* [Online]
Available at: http://ec.europa.eu/research/energy/eu/index_en.cfm?pg=research-wind
[Accessed 6 Februari 2014].

Gasch, R. & Twele, J., 2012. *Wind Power Plants: Fundamentals, Design, Construction.* Second Edition ed. s.l.:Springer Berlin Heidelberg.

Göransson, F. & Nordenmark, A., 2011. *Fatigue Assessment of Concrete Foundations for Wind Power Plants,* Göteborg: Chalmers Reproservice / Department of Civil and Environmental Engineering.

Olsson, K. & Pettersson, J., 2010. *Fatigue Assessment Methods for Reinforced Concrete Bridges in Eurocode,* Göteborg: Chalmers University of Technology.

PAGEL Spezial-Beton, 2013. *V1 HF Super high strenght grout,* Essen: PAGEL Spezial-Beton.

Rempling, R., 2009. *Modelling of Concrete Subjected to Cyclic Loading,* Göteborg: Chalmers Reproservice.

Shah, S. P. & Mu, B., 2005. Fatigue behavior of concrete subjected to biaxial loading in the compression region. *Materials and Structures,* 38(3), pp. 289-298.

Swedish Energy Agency, 2013. *Vindkraftsstatistik 2012,* Eskilstuna: Energimyndigheten.

Thun, H., 2006. *Assessment of Fatigue Resistance and Strength in Existing Concrete Structures,* Luleå: LTH.

Veljkovic, M., 2014. *VINDFORSK IV.* Luelå, s.n.

Vestas Wind Systems A/S, 2010. *Foundation Loads,* Randers: Vestas Wind Systems A/S.